12-8-2022

Integrative Revision of Five Genera Type Species for Zoanthidea To Bridge the Parataxonomy Gap

Jacob Colbert
Nova Southeastern University

Thesis of
Jacob Colbert

Submitted in Partial Fulfillment of the Requirements for the Degree of

Master of Science
Marine Science

Nova Southeastern University
Halmos College of Arts and Sciences

December 2022

Approved:
Thesis Committee

Committee Chair: Timothy Swain, Ph.D.

Committee Member: Jose Lopez, Ph.D.

Committee Member: Andrew Bauman, Ph.D.

HALMOS COLLEGE OF ARTS AND SCIENCES

Integrative Revision of Five Genera Type Species for Zoanthidea to Bridge the Parataxonomy Gap

Jacob Colbert

Submitted to the Faculty of Halmos College of Arts and Sciences in partial fulfillment of the requirements for the degree of Master of Science with a specialty in:

Marine Science

Nova Southeastern University

December, 2022

Thesis Advisor: Timothy Swain, Ph.D.

Committee Member: Jose Lopez, Ph.D.

Committee Member: Andrew Bauman, Ph.D.

Abstract

Cnidarian order Zoanthidea is a relatively understudied group of invertebrates inhabiting a diverse range of marine habitats. Over/During the last two decades, species descriptions within this order have largely been based on a novel molecular parataxonomic system that relies almost exclusively on DNA barcodes to detect and describe new species. DNA barcodes are short, conserved sequences that are readily compared across taxa and used to detect previously described species. The existing taxonomic system, based on anatomical analysis and the identification of evolutionarily informative characters for phylogenetic inference, has been recently replaced by molecular parataxonomy by some scientists/researchers. While molecular sequence data has been critical in quickly identifying new species of Zoanthidea, the sole reliance on a single source of information to describe species and infer evolutionary relationships falls short of modern taxonomic standards and practices. This research revisited the molecular parataxonomic species descriptions of five genera-type species within the Zoanthidea. Formal genus and species descriptions for *Kulamanamana haumeaae, Zibrowius ammophilus, Hurlizoanthus parrishi, Kauluzoanthus kerbyi,* and *Bullagummizoanthus emilyacadiaarum* were expanded to include microanatomical character analyses. Each type-specimen was found to exhibit the cyclically transitional marginal musculature arrangement as predicted by previous analyses. A comprehensive phylogenetic analysis was not achieved, due to the failure in extracting genetic material from the type specimens. The rationale for creating five monospecific genera (Sinniger *et al.*, 2013) was examined by mapping physical characters onto a redrawn phylogeny (Carreiro-Silva *et al*., 2017; Swain, 2018). Despite the specious reasoning of the original rationale for the erection of five monospecific genera, these genera names remain valid in the absence of additional molecular data from the type specimens.

Keywords: Cnidaria, Zoanthidea, Molecular Parataxonomy, Integrative Systematics, Histology

Acknowledgments

Funding for this research was provided by the President's Faculty Research and Development Grant. I would like to thank Dr. Timothy Swain for his continued support, patience, and indispensable expertise as my primary thesis advisor. This project would not have been possible without him. Additionally, I would like to thank my committee members Dr. Jose Lopez and Dr. Andrew Bauman for their time and expertise. I would also like to thank Dr. Abigail Renegar for her generosity in allowing me access and use of some of her laboratory equipment. Thank you to my wonderful uncles, George and Eduardo for supporting me throughout my stay in South Florida. Thank you to my wonderful parents for their continued encouragement and support. Lastly, I would like to thank my wife, Rachel, for going on this journey with me over the last two and a half years.

Table of Contents

List of Figures

List of Tables

Introduction

The cnidarian (Class: Anthozoa) order Zoanthidea is a group of invertebrate organisms inhabiting a wide range of benthic marine habitats, spanning shallow coral reefs to abyssal cold seep environments (Reimer *et al.*, 2007). Zoanthideans, specifically members of the suborder Macrocnemina, are colonial organisms that frequently participate in symbiotic relationships with a diversity of invertebrate host organisms, most commonly representatives of the Alcyonacea, Antipatharia, Hydrozoa, Demospongiae, Hexactinellida, and Paguridae (Swain, 2010; Ryland *et al.*, 2004). The specificity of symbiotic relationships across Zoanthidea taxa is often indicative of higher taxonomic relationships within the order and provides new information regarding the evolutionary history of symbioses (Swain & Wulff, 2007; Swain, 2010). The diversity of symbiotic relationships observed is conducive to the extensive geographical and bathymetric distributions of zoanthideans (Swain, 2010). Resembling the appearance of sea anemones (Cnidaria, Actiniaria), these epizoic animals are characterized by their polyp morphology: a cylindrical body column, attached at the bottom to colonial connective tissue, with the top of the polyp consisting of a flat oral disk with rows of tentacles lining the margins. Polyp retraction in Zoanthidea serves as a crucial startle-response protective behavior, and is achieved by recruiting multiple muscle groups, most notably the marginal musculature (consisting of varying muscle attachment and structural features across taxa) of the polyp (Swain *et al.*, 2015). Swain *et al.* (2015) demonstrated the diversity of polyp retraction mechanisms within the order, expanding the known marginal musculature forms from two to ten, reflective of a complex evolutionary history of Zoanthidea functional morphology.

Despite evidence of widespread distribution and a complex evolutionary history of zoanthideans, this order remains understudied. The true diversity within the order is largely unknown, partly due to the enigmatic nature and morphological plasticity of zoanthideans (Reimer *et al.*, 2006), and the difficulty of sampling and preserving specimens. Appletans *et al.* estimated that ~200–300 species have been formally described, with close to an anticipated 1,170 undescribed species. A scarcity of taxonomic and systematic specialists has largely led to Zoanthidea systematics remaining at an incipient stage. This has resulted in a lack of understanding of evolutionary relationships of species and higher taxa (genera, families) within the order. However, in the last two decades, a significant effort has been made to expand our

knowledge of the evolutionary history of Zoanthidea and contextualize this group within a comprehensive phylogenetic framework. Traditionally, Zoanthidea taxonomy and systematics research was conducted using classical anatomic methods (Schmidt, 1862; Abel, 1959) that examine the microanatomical features of the animal, identifying specific characters to differentiate Zoanthidea species and infer evolutionary relationships between higher taxa. However modern Zoanthidea systematics has become inundated with ill-informed gene trees that rely almost exclusively on molecular parataxonomic characters to infer phylogenetic relationships. This novel method relies on DNA barcoding data to detect, differentiate, and describe unknown Zoanthideans (Brower, 2006; Swain *et al.*, 2017). DNA barcodes are short, conserved DNA sequences that are readily compared across taxa and are typically used to detect species that have already been described. Through the recently extensive application of molecular parataxonomy to the order Zoanthidea, over 100 phylogenetic trees focused on Zoanthidea have been published since 2004 (Swain, 2018). Despite this, our understanding of the evolutionary relationships within the order have not progressed similarly. The overwhelming majority of the recently published phylogenetic trees within the order have been misinterpreted as species trees. Based solely on DNA barcoding data, often from a single gene, these phylogenetic trees are gene trees, reflecting the evolution of genes rather than of species (Swain, 2018).

Using DNA barcode data as the primary or sole source of evidence in phylogenetic reconstruction and species description disregards the basic principles of modern taxonomic and systematic practices, which dictate that phylogenetic hypotheses are informed through multiple lines of evidence (Lipscomb *et al.*, 2003; Vogler & Monaghan, 2007; Collins & Cruickshank 2013). The prominence of molecular parataxonomy within Zoanthidea systematics has also led to two competing taxonomic systems. Species described using the classic anatomically based system have no discernable meaning in molecular parataxonomic terms because these two systems share no characters with one another. Theoretically, taxa defined using solely molecular data cannot be verified as being different from previously described species in the existing taxonomic system, rendering over 150 years of previous research unusable. Additionally, DNA barcodes contain limited information and provide no insight relative to the form and function of specific characters. Consequently, characters generated from molecular parataxonomic

descriptions are not useful beyond the detection of described species and are largely uninformative for phylogenetic inference. Thus, over a decade of inferring evolutionary relationships from nucleotide sequences has illustrated a fundamental misunderstanding of the evolution of form in Zoanthidea (Sinniger *et al.*, 2005; Swain, 2010; Swain *et al.*, 2017). The molecular parataxonomic method also relies on a genetic sequencing technology that is not universally accessible to all scientists and cannot be applied to all previously collected specimens due to varying preservation protocols (Zamani *et al.*, 2022). While molecular techniques have been paramount in advancing our understanding of evolutionary relationships within the Zoanthidea and informing phylogenetic hypotheses, the extensive application of molecular parataxonomy to species descriptions and disregard for previously collected anatomical data has led to questionable classification conclusions in the Zoanthidea.

Sinniger *et al.* (2013) examined the diversity and evolutionary relationships of Hawaiian deep sea Zoanthidea and described five novel genera type species in the order Zoanthidea (*Kulamanamana haumeaae, Zibrowius ammophilus, Hurlizoanthus parrishi, Kauluzoanthus kerbyi, Bullagummizoanthus emilyacadiaarum*). A phylogenetic tree was constructed using concatenated mitochondrial 16S rDNA, mitochondrial cytochrome oxidase subunit 1 (COI), and nuclear 18S rDNA sequencing data. Each new species was assigned to its own new genus, based on insertion and deletion patterns within the V5 region of the mt16S rDNA gene. With only a perfunctory exploration of morphological characters that traditionally define Zoanthidea systematics, the descriptions presented by Sinniger *et al.* (2013) are based almost entirely on DNA barcodes. It has been demonstrated that within class Anthozoa, the rate of evolution of the COI gene is exceptionally slow and is insufficient at distinguishing between closely related species, as well as addressing phylogenetic questions below the genus-level (Shearer *et al.*, 2002). Additionally, analyses that include genes with divergent hypervariable regions, such as sequence data from mitochondrial 16S rDNA, tend to limit the scope of research to closely related species in order to avoid difficult homology assessments, as is the case in this study (Swain, 2018). Several genes, such as the nuclear ITS2, 5.8S, ITS2, 28S, and mitochondrial 12S, were not included in the molecular approach by Sinniger *et al.* (2013), even though these genes are widely used in zoanthidean phylogenetics prior to this publication. Therefore, the phylogenetic assessment conducted by Sinniger *et al.* (2013) can be expanded and the phylogeny

improved. These specimens also lack an extensive morphological analysis (i.e., no longitudinal or transverse serial sections examining internal morphology). Therefore, further investigation regarding the evolutionary relatedness, morphology, and classifications of the mentioned Zoanthidea taxa is warranted.

In the Northeast Atlantic region of the Azores, an epizotic zoanthidean associated with the cold-water gorgonian *Callogorgia verticillate* was described (Carreiro-Silva *et al.*, 2011). This new species description, originally named *Isozoanthus primnoidus*, was largely based on various morphological and anatomical characters of the polyps and cnidae type (Carreiro-Silva *et al.*, 2011). Forming symbiotic relationships with primnoid octocorals, *Isozoanthus primnoidus* was reevaluated following the publication of Sinniger *et al.* (2013) and it was determined that this species belonged in the genus *Zibrowius*, based on the molecular analysis of Sinniger *et al.* (2013). In the same study, another zoanthidean associated with primnoid octocorals was described and placed in the genus *Hurlizoanthus*. The two species, *Hurlizoanthus hirondelleae* and *Zibrowius primnoidus*, were placed within a phylogenetic context using concatenated mitochondrial COI, 16S, and 12S genes. As previously stated, mitochondrial COI genes are uninformative at the genus and species level. The genetic analysis conducted by Carreiro-Silva *et al.* (2017) can also be expanded by sequencing nuclear genes of the ITS region. Longitudinal and transverse serial sections are also unavailable for these two specimens, meaning that their species descriptions are heavily reliant on DNA barcodes and are isolated from the existing taxonomic system. In order to incorporate these species hypotheses within a larger phylogenetic framework, these two species require comprehensive revision.

The most comprehensive phylogeny of the Zoanthidea to date was published by Swain (2018). This phylogeny placed the five genera erected by Sinniger *et al.* (2013) in close relation to genera *Savalia* and *Corallizoanthus* (Figure 1). Because of the highly conserved evolution of marginal musculature form (Swain *et al.*, 2015), the marginal musculature of *Savalia* and *Corallizoanthus* should be predictive of the marginal musculature of the Sinniger *et al.* (2013) genera. Swain *et al.* (2015) determined through histological serial sectioning that both *Savalia* and *Corallizoanthus* have cyclically transitional marginal musculature arrangements This type of marginal musculature consists of cyclical transitions between mesogleal pleats and

mesogleal lacunae. This expansion of the morphological analysis could offer a key feature for modern systematics within an order where higher taxa largely lack definitive feature descriptions, due to being defined by molecular parataxonomy (Swain *et al.*, 2015).

Molecular data has been paramount in exposing the shortcomings of historical morphology-based systematics in the Zoanthidea (i.e., morphological features that had defined taxa were homoplastic and did not circumscribe clades delineated by ecological and molecular characters (Swain *et al.*, 2017)). Challenges with morphology-based systematics in the Zoanthidea remain, however molecular taxon species definitions within the Zoanthidea are disconnected from the existing form-based systematics (Vogler & Monaghan 2007) and will eventually require revision before they can become useful or discredited (Will *et al.*, 2005; Pante *et al.*, 2015).

The primary aim of the research presented here is to apply an integrative systematic approach, expanding on the molecular and morphological analysis of Sinniger *et al.* (2013) for the five genera-type species. Histological analysis was performed on type specimens from the United States National Museum of Natural History (USNM). Longitudinal and transverse sections were created, documented, and measured to assess marginal musculature arrangements and other important microanatomical features. Enhanced molecular phylogenetic analyses were attempted by targeting an additional five nuclear genes (18S, ITS1, 5.8S, ITS2, & 28S) and two mitochondrial genes 12S & 16S) from USNM type specimens that were submitted as genetic vouchers with the goal of improving resolution of the seven aforementioned species in the Zoanthidea phylogeny.This integrative approach will simultaneously help to bridge the parataxonomic gap by reintegrating the target species and genera into the existing taxonomic system and improving the resolution and certainty in our phylogenetic inference of the order Zoanthidea.

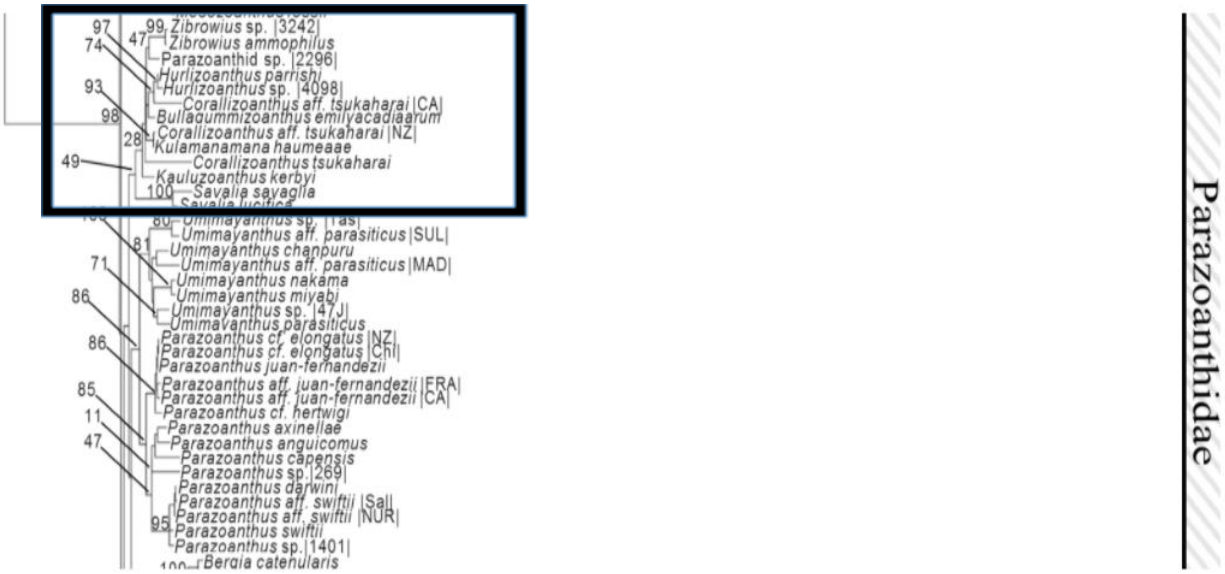

Figure 1. Portion of Zoanthidea phylogeny generated by Swain (2018). Phylogeny based on concatenated 18S, ITS, 5.8S, 28S, mt 12S, and mt 16S genes using a staggered alignment. Support indicated by 1000 pseudoreplicated maximum likelihood bootstrap values. The five genus type species described in Sinniger *et al.* (2013), *Corrallizoanthus*, and *Savalia* are located within the black-bordered box.

Materials & Methods

Sample Acquisition:

Zoanthidea type specimens for *Kulamanamana haumeaae* (Formalin-fixed, USNM 1190187; Ethanol-fixed, USNM 1190188), *Zibrowius ammophilus* (Formalin-fixed, USNM 1190191; Ethanol-fixed, USNM 1190192), *Hurlizoanthus parrishi* (Formalin-fixed, USNM 1190193; Ethanol-fixed, USNM 1190194), *Kauluzoanthus kerbyi* (Formalin-fixed, USNM 1190195, Ethanol-fixed), *Bullagummizoanthus emilyacadiaarum* (Formalin-fixed, USNM 1190197; Ethanol-fixed 1190198) were loaned from the United States National Museum of Natural History. These specimens were originally collected from deep slopes and seamounts of the Hawaiian Archipelago (Sinniger *et al.*, 2013). All specimens were stored in 95% ethanol at −80°C in the Evolution of Marine Symbioses Laboratory at the Nova Southeastern University Guy Harvey Oceanographic Center.

Attempts to obtain the type specimens for *Zibrowius primnoidus* and *Hurlizoanthus hirondelleae* (Carreiro-Silva *et al.*, 2017) from the COLETA Reference Collection of the

Department of Oceanography and Fisheries, University of the Azores (DOP-Uaz) were unsuccessful. We had been in positive communication via email with Marina Parra Carreiro e Silva for several months, but eventually they became unresponsive and the timeframe where the specimens could be used in this thesis expired.

Histology:

Four individual polyps were removed from each specimen (two for longitudinal sectioning; two for transverse sectioning) and underwent decalcification to dissolve embedded materials (foraminifera tests, basalts, sclerites, etc.) from the polyp column wall. Acid digestion consisted of decalcification in Formical-4 (Formic acid and formalin) for 4 hours (x2), rinsing with distilled water, and desilicification in 20% hydrofluoric acid for 8–24 hours. Following desilicification, polyps were rinsed with distilled water and stored in 70% ethanol.

Polyps were hand cut with a razor blade in order to expose internal structures to paraffin. Prior to paraffinization, polyps were dehydrated and cleared in xylene in microcentrifuge tubes. Polyps were dehydrated in 80% ethanol for 10 minutes, followed by 90% ethanol for 15 minutes (x2), followed by 100% ethanol for 20 minutes (x3). Polyps were then suspended in xylene for 25 minutes (x4). One ml of paraffin was added to the mixture and polyps were incubated at 56°C overnight. Following ~24 hour incubation, the xylene/paraffin mixture was replaced with pure paraffin and incubated at 56°C. Paraffin replacement was repeated two more times, occurring once per hour. Polyps were then moved to plastic molds and filled with melted paraffin. Polyps were oriented horizontally (for transverse sectioning) or parallel (for longitudinal sectioning) to the base of the plastic mold using heated forceps. Paraffin blocks were then chilled overnight.

Histological sectioning was done using a Leica RM2125 RTS microtome. Paraffin wax blocks containing individual polyps were mounted onto the microtome and cut in 10µm thick sections. Sections were then placed in sequence onto poly-L-lysine glass slides. Slides with sections were then deparaffinized with xylene. Following deparaffinization, slides were then stained using Harris' hematoxylin and eosin-Y (H&E staining) following methods by Swain (2009). Stained slides were dehydrated using 95% and 100% ethanol and cleared once more in

xylene. A coverslip was then mounted to each slide using Permount, a toluene-based synthetic resin. Completed slides were then dried overnight. The complete staining procedure can be found in Swain (2009). Stained slides were viewed and photographed using a Leica DM2500 LED compound microscope with a digital camera and Leica LAS-X image acquisition and analysis software.

Measurements from transverse (cross) and longitudinal sections followed protocols outlined in Swain (2009) and Swain *et al.* (2015). Measurements were taken from sections that captured the regions of interest (at the height of actinopharynx for transverse sections, marginal musculature for longitudinal sections). For each specimen, ten serial sections were photographed for both longitudinal and transverse sections. For transverse sections, characters of interest included the ventral directive length and width, microneme length and width, siphonoglyph mesoglea thickness, siphonoglyph endoderm thickness, siphonoglyph ectoderm thickness, column mesoglea thickness, column endoderm thickness, and column ectoderm thickness (Figure 2). For longitudinal sections, characters of interest included the length of the marginal muscle, length of the longest pleat (muscle attachment), diameter of the marginal muscle, and the surface area of the marginal musculature (Figure 3). Additionally, photographs of the marginal musculature were taken in sequence for each specimen, displaying the transitional states of cyclically transitional marginal musculature arrangements from mesogleal pleats to mesogleal lacunae. Measurements of each character, measured in micrometers (µm), were made using the Leica LAS-X software application.

Figure 2. Cross section of *Hurlizoanthus parrishi*, showing (A) siphonoglyph endoderm, (B) siphonoglyph mesoglea, (C) siphonoglyph ectoderm, (D) ventral directive, (E) microneme, (F) column endoderm, (G) column mesoglea, and (H) column ectoderm.

Figure 3. Longitudinal section of *Zibrowius ammophilus* showing (A) mesogleal pleat, (B) marginal musculature, (C) mesogleal lacunae.

DNA Extraction

Total genomic DNA was extracted from each specimen following the CTAB (cetyltrimethyl-ammonium bromide) technique outlined in Doyle & Doyle (1987). 200µL of CTAB was added to a 1.5ml microcentrifuge tube, followed by 2.5µl of Proteinase K (10mg/ml). Zoanthidea tissues were grinded and mixed, then incubated at 60°C for one hour while being shaken using a rocker. 400µl of CIA (chloroform isoamyl alcohol at a 24:1 ratio) was added to the mixture under a fume hood. Without disturbing the interface, the upper aqueous phase was removed and added to a new 1.5ml microcentrifuge tube. 200µl of 95% ethanol (refrigerated at −20°C) was added to the mixture and mixed by inverting the microcentrifuge tube. The mixture was precipitated at −20°C for a minimum of one hour. Following precipitation, the microcentrifuge tube was centrifuged for 10 minutes at 10,000 × g with the tube hinges facing outwards. Following centrifugation, ethanol was removed from the tube without disturbing the

DNA pellet. 1ml of 70% ethanol (stored at −20°C) was used to wash the pellet. The tube was then centrifuged for an additional 10 minutes at 16,000 × g with the tube hinges facing outward. The remaining ethanol was again removed without disturbing the pellet. The DNA pellet was then dried at 45°C in an incubator until the remaining ethanol had dissipated. The DNA pellet was then resuspended in 50µl of TE buffer. Extractions were diluted in molecular grade water to approximately 20ng/µl.

An additional DNA extraction protocol was attempted based on the procedure for DNA extraction from formalin-fixed paraffin embedded medical specimens following Nguyen *et al.* (2021). The extraction protocol is intended to partially reverse formaldehyde modification of nucleic acids from formalin-fixed specimens through extended proteinase digestion and heat shock. Heating at high temperature (94°C) at an alkaline pH (pH = 8.0) has been shown to be crucial for improving the quantity and quality of the extracted DNA by reversing the crosslinking between nucleic acids and proteins (Nguyen *et al.* 2021). This required additional incubation periods following the addition of 200µl of CTAB and 2.5µl Proteinase K (10mg/ml) to a 1.5ml microcentrifuge tube as outlined above. Tissues were grinded and mixed, then incubated at 60°C for three hours while being shaken using a rocker. Tissues were then incubated at 94°C for one hour and then allowed to cool to room temperature. 400µl of CIA (24:1 ratio) was added to the mixture under a fume hood. The mixture was then centrifuged for 10 minutes at 13,000 × g at room temperature under the fume hood. Following centrifugation, the upper aqueous phase was removed without disturbing the pellet and transferred to a new 1.5ml microcentrifuge tube. 200µl of 95% ethanol (stored at −20°C) was added to the tube, mixed by inversion, and precipitated at −20°C overnight. Following precipitation, samples were centrifuged in a refrigerator for 10 minutes at 10,000 × g with the tube hinges facing outwards. Following centrifugation, ethanol was removed from the tubes without disturbing the DNA pellet. Pellets were washed with 1ml of 70% ethanol (stored at −20°C). Samples were then centrifuged in a refrigerator for 10 minutes at 16,000 × g with the tube hinges facing outward. Ethanol was removed from each tube without disturbing the pellets and dried at 45°C in an incubator until the remaining ethanol had dissipated. DNA pellets were then resuspended in 20µl of molecular grade water. Samples were not diluted following suspension in an attempt to concentrate any DNA extracted.

PCR Amplification

Table 1. Table includes target genes and primer sequences used in attempts to amplify DNA sequences for phylogenetic analysis.

Gene	Primer	Sequence	Annealing Temperature	Fragment Size (bp)	Primer Source
ITS	ITS-f ITS-r	CTAGTAAGCGCGAGTCATCAGC GGTAGCCTTGCCTGATCTGA	50°C	770– 943	Swain 2009
18S	18S-Zoan f 18S-Zoan r	GCGAATGGCTCATTAAATCAGTTATCG CTTTGCAACCATACTTCCCCCGGAACC	60°C		Sinniger *et al.* 2013
16S	antla-f bmoH-r	GCCATGAGTATAGACGCACA CGAACAGCCAACCCTTGG	50°C	835– 889	Sinniger *et al.* 2005

Polymerase chain reaction (PCR) amplification attempts were performed in order to target and amplify ITS1, ITS2, 18S, 16S, and 12S genetic markers. A description of genes targeted and primers used can be found in Table 1. Despite multiple PCR and extraction attempts, no success was made in producing sequence-able PCR products for any of the five Zoanthidea species. No attempts were made to amplify 28S genes or mitochondrial 12S rRNA genes due to the exhaustion of sample material.

To amplify ITS rRNA nuclear genes, primers ITSf and ITSr were used (Swain, 2009). The thermal protocol used was: 95°C for 3 minutes, 95°C for 45 seconds, 50°C for 60 seconds, 72°C for 75 seconds (repeated 37x for a total of 38 cycles), followed by a final extension step of 72°C for 8 minutes. Two attempts to amplify targeted ITS regions were unsuccessful, indicated by no detection of PCR products in standard agarose gel electrophoresis.

To amplify mitochondrial 16S genes, primers 16S-ant1aF and 16S-bmoHr were used (Sinniger *et al.*, 2005). The thermal protocol used was: 95°C for 3 minutes, 95°C for 45 seconds, 50°C for 60 seconds, 72°C for 75 seconds (repeated 37x for a total of 38 cycles), followed by with a final extension step of 72°C for 8 minutes. Two attempts to amplify targeted mitochondrial 16S regions were unsuccessful, indicated by no detection of PCR products in standard agarose gel electrophoresis.

To amplify nuclear 18S genes, primers 18S-ZoanF and 18S-ZoanR were used (Swain, 2009). The thermal protocol used was: 95°C for 3 minutes, 95°C for 45 seconds, 60°C for 60 seconds, 72°C for 75 seconds (repeated 37x for a total of 38 cycles), followed by a final extension step of 72°C for 8 minutes. Two attempts to amplify targeted nuclear 18S regions were unsuccessful, indicated by no detection of PCR products in standard agarose gel electrophoresis.

Results

Taxonomy

Suborder Macrocnemina Haddon & Shackleton, 1891

Zoanthidea with perfect fifth mesenteries (Haddon & Shackleton 1891). Perfect fifth mesenteries, the defining character for the suborder Macrocnemina, is plesiomorphic. The suborder Macrocnemina is paraphyletic with respect to the suborder Brachynemina (Sinniger *et al.*, 2010; Swain & Swain, 2014).

Family Parazoanthidae Delage & Hérouard, 1901

Zoanthidea with macrocnemic mesenterial arrangement and simple endodermal marginal musculature (Delage & Hérouard, 1901); excluding species that form a monophyly with Brachynemina (Sinniger *et al.*, 2010; Swain, 2010).

Genus *Kulamanamana* Sinniger in Sinniger, Ocana & Baco, 2013

Type species. *Kulamanamana haumeaae* Sinniger in Sinniger, Ocana & Baco, 2013, by original designation.

Diagnosis. Macrocnemic genus associated with octocorals and the secretion of a scleroproteic skeleton. Absence of mineral incrustations in the ectoderm, well developed coenenchyme completely covering the host. Characteristic insertion/deletion pattern in the 16S V5 mitochondrial region, located in the second half of the mt16S rDNA gene (original diagnosis of Sinniger *et al*., 2013). Marginal musculature cyclically transitional, 646–733 μm in length, composed of 9–27 attachment points (diagnosis expanded using data presented here).

Remarks. Creation of *Kulamanamana* largely based on a characteristic insertion/deletion pattern in the mt 16S V5 region and the secretion of a golden to dark brown sclereoproteic skeleton (Sinniger *et al.*, 2013). The original diagnosis has been expanded to include the arrangement of the marginal musculature (cyclically transitional). According to the original description of the family Parazoanthidae, taxa within this family are said to have simple

endodermal marginal musculature (Delage & Hérouard, 1901). This is in direct contradiction with the findings of this research. Therefore, revision of Parazoanthidae is warranted.

***Kulamanamana haumeaae* Sinniger in Sinniger, Ocana & Baco, 2013**

Figure 4–5. Morphobank species collection F1079

Material examined. USNM 1190187, holotype.

Diagnosis. *Kulamanamana* with cyclically transitional marginal musculature; marginal muscle up to 733 µm in length ($\bar{x}$ = 686 µm, nsections = 10), composed of as many as 27 muscle attachment points ($\bar{x}$ = 18, nsections = 47). Mesenterial arrangement macrocnemic (Sinniger et al., 2013). Golden axis, tissue color ranging from a pale yellow to medium orange, secretion of excessive mucus when collected and the absence of mineral incrustations are distinct characters of the species (Sinniger et al., 2013). Occurring at 343–544m in the western Pacific (Hawaii), symbiotic primarily with isidid octocorals though no host preference has been determined (Sinniger et al., 2013). To date, similar specimens referred to as "Gerardia" have been collected in the West Atlantic and in New Zealand (Sinniger et al., 2013).

Description. Colony. Coenenchyme completely covering the host (Sinniger *et al.*, 2013). In vivo, polyps, tentacles and coenenchyme bright yellow to dark orange (Sinniger *et al.*, 2013). Polyp density variable throughout colony with coenychyme barely visible in most dense regions and separated by over 1 cm in least dense regions (Sinniger *et al.*, 2013). Golden scleroproteic skeleton distinct from black skeleton in the genus *Savalia* (Sinniger *et al.*, 2013). Bioluminescence observed *in situ* (Sinniger *et al.*, 2013).

Polyp. In preserved specimens, contracted polyps 1–8 mm in length, 2–7 mm in diameter (Sinniger *et al.*, 2013). 28–31 tentacles (Sinniger *et al.*, 2013). Column cylindrical with no encrustations.

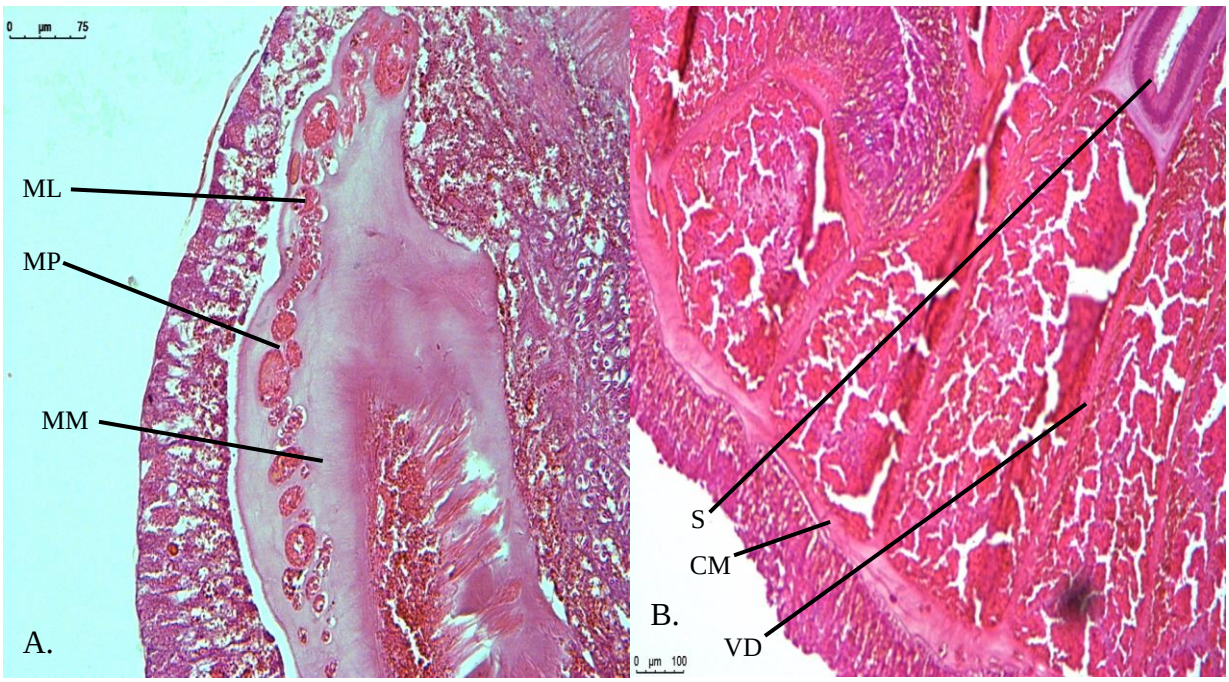

Figure 4. Histology of *Kulamanamana haumeaae* (10 µm sections). **A.** Longitudinal section showing marginal musculature (MM), mesogleal pleat (MP) and mesogleal lacunae (ML). **B.** Transverse (cross) section displaying a single siphonoglyph (S), column mesoglea (CM), and ventral directive (VD).

Internal Anatomy. Azooxanthellate (Sinniger *et al.*, 2013). In longitudinal sections (Morphobank collection F1079), marginal musculature cyclically transitional with a period of approximately 230 µm per transition (Figure 5). Muscle fibers contained within 0–22 ($\overline{x}$ = 7, $n_{sections}$ = 47) mesogleal lacunae (Figure 4A.) that span entire mesoglea distally; lacunae restricted to endoderm proximally, with most-proximal lacunae opening to endoderm and forming 9–27 ($\overline{x}$ = 18, $n_{sections}$ = 47) mesogleal pleats (Figure 4A.). Length of marginal musculature (Figure 4A.) 645–733 µm ($\overline{x}$ = 686 µm, $n_{sections}$ = 10); diameter of muscle at widest point (Figure citation) 42–77 µm ($\overline{x}$ = 53 µm, $n_{sections}$ = 10).

In cross sections at the actinopharynx (Morphobank collection F1079), mesenteries follow macrocnemic arrangement with a single siphonoglyph (Figure 4B). Thickness of siphonoglyph ectoderm ranged from 27–55 µm ($\overline{x}$ = 36 µm, $n_{sections}$ = 10). Thickness of siphonoglyph mesoglea ranged from 11–27 µm ($\overline{x}$ = 19 µm, $n_{sections}$ = 10). Thickness of siphonoglyph endoderm 12–55 µm ($\overline{x}$ = 27 µm, $n_{sections}$ = 10). Adjacent siphonoglyph, column ectoderm thickness 166–329 µm ($\overline{x}$ = 235 µm, $n_{sections}$ = 10), mesoglea thickness 48–109 µm ($\overline{x}$ = 68 µm, $n_{sections}$ = 10), and endoderm thickness 18–81 µm ($\overline{x}$ = 40 µm, $n_{sections}$ = 10). Microneme

20–135 µm in length ($\bar{x}$ = 68 µm, $n_{sections}$ = 10), 14–53 µm in width ($\bar{x}$ = 31 µm, $n_{sections}$ = 10). Ventral directives supported by mesoglea 532–833 µm ($\bar{x}$ = 670 µm, $n_{sections}$ = 10) from column to siphonoglyph, 11–39 µm ($\bar{x}$ = 19 µm, $n_{sections}$ = 10) width. Encircling sinus absent (Figure 4B).

Cnidae. Mesenterial filaments contain spirocysts, spirulae (b-mastigophores, basitrichs), and small homotrichs (holotrichs) (Sinniger et al., 2013).

Distribution. Found throughout the Hawaiian Archipelago seamount and island slopes between 343–575 m on hard substrata in low sediment areas (Sinniger *et al.*, 2013). Also observed in Line and Jarvis Islands, Palmyra Atoll and Kingman Reef (Sinniger *et al.*, 2013).

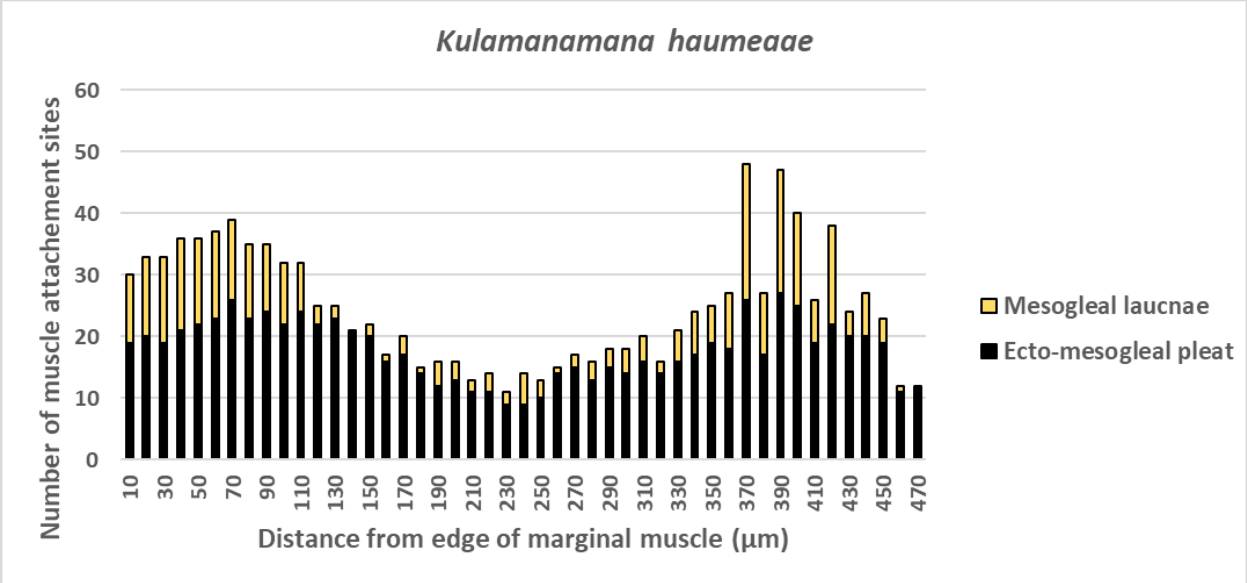

Figure 5. Number, position, and type of marginal muscle attachment sites as they appear in serial longitudinal sections of *Kulamanamana haumeaae*. Individual columns represent a 10 µm longitudinal section with the number and type of muscle attachment points; black bars indicate ectodermal-mesogleal pleats, yellow bars indicate mesogleal lacunae.

Remarks. The original description of *Kulamanamana haumeaae* did not report on the arrangement of the marginal musculature. The microanatomical analysis of *K. haumeaae* in Sinniger *et al.* (2013) lacks longitudinal and transverse serial sectioning. It appears that when viewing longitudinal serial sections of *K. haumeaae* in sequence, the marginal musculature arrangement of the species can be described as cyclically transitional, consisting of a cyclic continuum of ectodermal-mesogleal pleats to a combination of ectodermal-mesogleal pleats and mesogleal lacunae, over a transition period of approximately 230 µm (Figure 5). This type of marginal musculature is congruent with the marginal musculature of species within the genera

Corallizoanthus (Swain, 2010; Swain & Swain, 2014) and similar to that of *Savalia savaglia* (Swain *et al.*, 2015).

Genus *Zibrowius* Sinniger in Sinniger, Ocana & Baco, 2013

Type species. *Zibrowius ammophilus* Sinniger in Sinniger, Ocana & Baco, 2013, by original designation.

Diagnosis. Sand incrusted, arborescent fan shaped colonies, golden skeleton. Well-developed coenenchyme covering host, can be confused with *Kulamanamana*, distinguishable by the presence of sand in the ectoderm, characteristic insertion/deletion pattern in the 16S V5 mitochondrial region located in the second half of the mt16S rDNA gene (original diagnosis of Sinniger *et al.*, 2013). Marginal musculature cyclically transitional, 541–604 μm in length, composed of 12–25 attachment points (diagnosis expanded using data presented here).

Remarks. *Zibrowius* was created based on sand incrustations in the ectoderm, golden skeleton, and a characteristic insertion/deletion pattern in the mt 16S V5 region (Sinniger *et al.*, 2013). The original diagnosis has been expanded to include the arrangement of the marginal musculature (cyclically transitional). According to the original description of the family Parazoanthidae, taxa within this family are defined as having simple endodermal marginal musculature (Delage & Hérouard, 1901). This is in direct contradiction with the findings of this research. Therefore, revision of Parazoanthidae is warranted.

***Zibrowius ammophilus* Sinniger in Sinniger, Ocana & Baco, 2013**

Figure 6–7. Morphobank species collection F1086

Material examined. USNM 1190191, holotype.

Diagnosis. *Zibrowius* with cyclically transitional marginal musculature; marginal muscle up to 604 μm in length ($\bar{x}$ = 586 μm, $n_{sections}$ = 10), composed of as many as 25 muscle attachment points ($\bar{x}$ = 17, $n_{sections}$ = 49). Mesenterial arrangement macrocnemic. Occurring at 389– 409m in the Western Pacific (Hawaii) with no known symbiotic host preferences (assumed to associate with octocorals based on external morphology and similarity of *Kulamanamana*

haumeaae; Sinniger *et al*., 2013). Golden axis, orange/brownish in color and presence of mineral encrustations are distinctive characters of this species (Sinniger *et al.*, 2013).

Description. Colony. Coenenchyme completely covering the host, polyp density variable within colony with coenechyme barely visible in densest regions and polyps separated by over 1 cm in less dense regions (Sinniger *et al.*, 2013). Golden scleroproteic skeleton, distinct from the black skeleton found in the genus Savalia (Sinniger *et al.*, 2013). It is unknown whether this species secretes its own skeleton due to rarity of the specimens (Sinniger *et al.*, 2013). Colony can spread to other substrata from the base of the original host (Sinniger *et al.*, 2013).

Polyp. In preserved specimens, size of polyps range from 1–5 mm in length and 1–3 mm in diameter, 20–33 tentacles (Sinniger *et al.*, 2013). Column cylindrical, with incrusted particles consisting of mainly basalt and foraminifera (Sinniger *et al.*, 2013). In vivo, polyps, tentacles and coenenchyme are brownish-yellow, resembling *Kulamanamana haumeaae* but distinct enough to be differentiated when viewed from the submersible (Sinniger *et al.*, 2013).

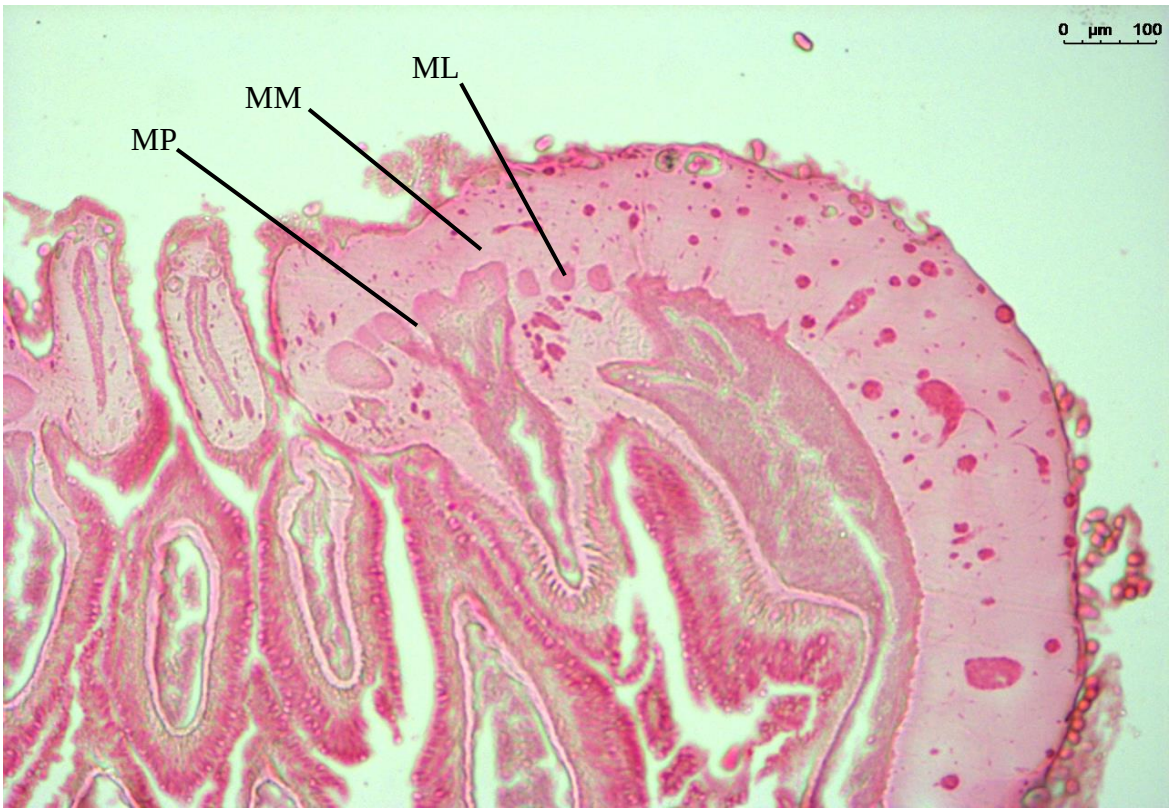

Figure 6. *Histology of Zibrowius ammophilus*. Longitudinal section showing marginal musculature (MM), mesogleal pleat (MP), and mesgleal lacunae (ML).

Internal Anatomy. Azooxanthellate, specimens analyzed were fertile (Sinniger *et al.*, 2013). In longitudinal sections (Morphobank collection F1086), marginal musculature cyclically transitional with a period of approximately 110–150 µm per transition (Figure 7). Muscle fibers contained within 0–21 ($\bar{x}$ = 10, $n_{sections}$ = 49) mesogleal lacunae (Figure 6) that span entire mesoglea distally; lacunae restricted to endoderm proximally, with most-proximal lacunae opening to endoderm and forming 12–25 ($\bar{x}$ = 17, $n_{sections}$ = 49) mesogleal pleats (Figure 6). Length of marginal musculature (Figure 6) 541–604 µm ($\bar{x}$ = 586 µm, $n_{sections}$ = 10); diameter of muscle at widest point (Figure 6) 103–142 µm ($\bar{x}$ = 125 µm, $n_{sections}$ = 10). Additional row of lacunae located near endoderm where muscle appears to be mesogleal (Figure 6) are a result of dissolved encrustations. Large lacunae throughout ectoderm and mesoglea resulting from dissolution of encrustations.

Cross sections at the actinopharynx of *Zibrowius ammophilus* were not obtained due to difficulty in sectioning and limited type material from USMN. The original description (Sinniger *et al.*, 2013) details the species having a small siphonoglyph that is not especially developed.

Cnidae. Mesenterial filaments contain spirocysts; spirulae; p-mastigophores; holotrichs (Sinniger *et al.*, 2013).

Distribution. To date, only collected on Hawaiian cross seamount (Sinniger *et al.*, 2013).

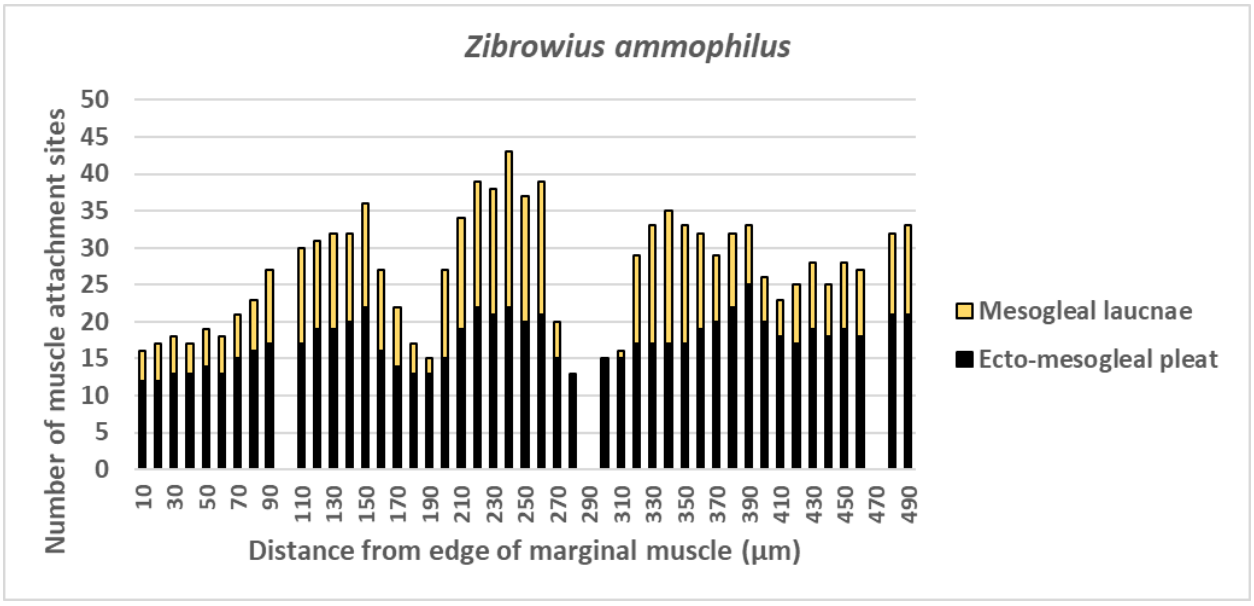

Figure 7. Number, position, and type of marginal musculature attachment sites as they appear in serial longitudinal sections of *Zibrowius ammophilus*. Individual columns represent a 10 µm longitudinal section with the number and type of muscle attachment points; black bars indicate ectodermal-mesogleal pleats, yellow bars indicate mesogleal lacunae. Empty positions indicate missing data due to sectioning artifact.

Remarks. The original description reports the marginal musculature as endodermal, short and concentrated in the upper part of the column (Sinniger *et al.*, 2013). The microanatomical analysis of *Z. ammophilus* in Sinniger *et al.* (2013) lacks longitudinal and transverse serial sectioning. When not viewed in serial sections, marginal musculatures in the cyclically transitional arrangement may often be misinterpreted as endodermal. It appears that when viewing longitudinal serial sections of *Z. ammophilus* in sequence, the marginal musculature arrangement of the species can be described as cyclically transitional, consisting of a cyclic continuum of ectodermal-mesogleal pleats to a combination of ectodermal-mesogleal pleats and mesogleal lacunae, over a transition period of approximately 110–150 µm (Figure 7). This type of marginal musculature is congruent with the marginal musculature of species within the genera *Corallizoanthus* (Swain, 2010; Swain & Swain, 2014) and similar to that of *Savalia savaglia* (Swain *et al.*, 2015).

Genus *Hurlizoanthus* Sinniger in Sinniger, Ocana & Baco, 2013

Type species. *Hurlizoanthus parrishi* Sinniger in Sinniger, Ocana & Baco, 2013, by original designation.

Diagnosis. Macrocnemic genus associated with primnoids, characteristic insertion/deletion pattern in the 16S V5 mitochondrial region located in the second half of the mt16S rDNA gene (original diagnosis of Sinniger *et al.*, 2013). Marginal musculature cyclically transitional, 482–588 µm in length, composed of 7–20 attachment points (diagnosis expanded using data presented here).

Remarks. *Hurlizoanthus* created largely based off characteristic insertion/deletion pattern in mt 16S V5 region with brief mention of host association. The diagnosis has been expanded to include the marginal musculature arrangement (cyclically transitional). According to the original description of the family Parazoanthidae, taxa within this family are said to have simple endodermal marginal musculature (Delage & Hérouard, 1901). This is in direct contradiction with the findings of this research. Therefore, revision of Parazoanthidae is warranted.

***Hurlizoanthus parrishi* Sinniger in Sinniger, Ocana & Baco, 2013**

Figure 8–9. Morphobank species collection F1085

Material examined. USNM 1190193, holotype.

Diagnosis. *Hurlizoanthus* with cyclically transitional marginal musculature; marginal muscle up to 588 µm in length ($\overline{x}$ = 546 µm, $n_{sections}$ = 10), composed of as many as 20 muscle attachment points ($\overline{x}$ =15, $n_{sections}$ = 56). Mesenterial arrangement macrocnemic. White color and few ramifications are distinctive characters of this species (Sinniger *et al.*, 2013). In the the cnidome, the prescence of big penicilli in the body wall appear to be characteristic of the species (Sinniger *et al.*, 2013). Occurring at 390–496m in the Western Pacific (Hawaii) colonizing unidentified octocorals of the family Primnoidae (original diagnosis of Sinniger *et al.*, 2013).

Description. Colony. Colony size reaching 30 cm height and 15 cm in diameter, no apparent branching beyond the host octocoral skeleton (Sinniger *et al.*, 2013). Coenenchyme thin and completely covering the host, white in color, always visible in between polyps (Sinniger *et al.*, 2013).

Polyp. Polyps 1-5 mm in length and 1-3 mm diameter, 30–35 tentacles, both polyps and tentacles white *in vivo* (Sinniger *et al.*, 2013). Column cylindrical with incrusted foraminifera and basalt particles (Sinniger *et al.*, 2013).

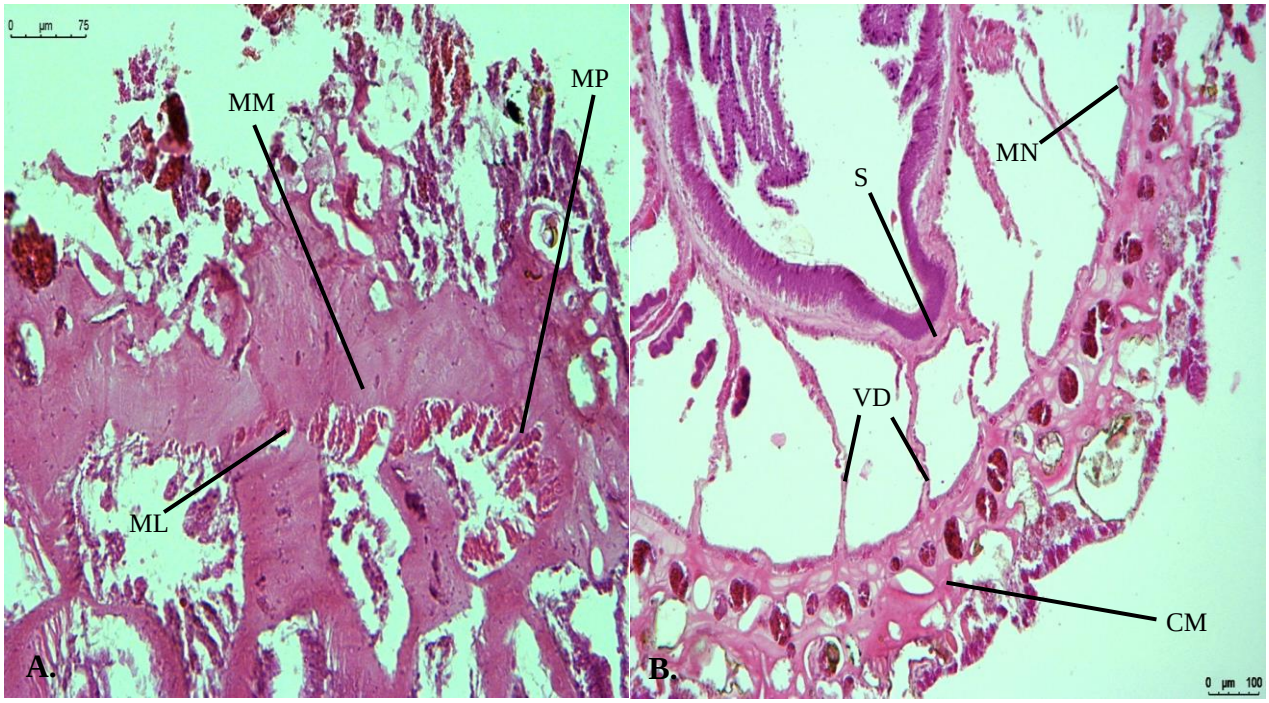

Figure 8. Histology of *Hurlizoanthus parrishi* (10 µm sections). **A.** Longitudinal section showing marginal musculature (MM), mesogleal pleat (MP) and mesogleal lacunae (ML). **B.** Transverse (cross) section showing a single siphonoglyph (S), column mesoglea (CM), ventral directive (VD) and microneme (MN).

Internal Anatomy. Azooxanthellate (Sinniger *et al.*, 2013). In longitudinal sections (Morphobank collection F1085)**,** marginal musculature cyclically transitional, with a period of approximately 110–140 µm (Figure 9). Muscle fibers contained within 0–16 ($\overline{x}$ = 7, $n_{sections}$ = 55) mesogleal lacunae (Figure 8A) that span entire mesoglea distally; lacunae restricted to endoderm proximally, with most-proximal lacunae opening to endoderm and forming 7–20 ($\overline{x}$ = 15, $n_{sections}$ =55) mesogleal pleats (Figure 8A). Length of marginal musculature (Figure 8A) 482–588 ($\overline{x}$ = 546 µm, $n_{sections}$ = 10); diameter of muscle at widest point (Figure 8A) 73–115 µm ($\overline{x}$ = 90 µm, $n_{sections}$ = 10). Additional row of lacunae located near endoderm where muscle appears to be mesogleal (Figure 8A) are a result of dissolved encrustations (foraminifera and basalt). Large lacunae throughout ectoderm and mesoglea resulting from dissolution of encrustations (Figure 8A).

In cross sections at the actinopharynx (Morphobank collection F1085), mesenteries follow macrocnemic arrangement with a single siphonoglyph (Figure 8B). Thickness of siphonoglyph ectoderm ranged from 25–47 µm ($\overline{x}$ = 39 µm, $n_{sections}$ = 10). Thickness of

siphonoglyph mesoglea ranged from 7–26 µm ($\bar{x}$ = 21, $n_{sections}$ = 10). Thickness of siphonoglyph endoderm 5–11 µm ($\bar{x}$ = 8, $n_{sections}$ = 10). Adjacent siphonoglyph, column ectoderm thickness 41–108 µm ($\bar{x}$ = 79 µm, $n_{sections}$ = 10), mesoglea thickness 84–175 µm ($\bar{x}$ =126 µm, $n_{sections}$ = 10), and endoderm thickness 18–25 µm ($\bar{x}$ = 21 µm, $n_{sections}$ = 10). Microneme 19–45 µm in length ($\bar{x}$ = 33 µm, $n_{sections}$ = 10), 6–23 µm in width ($\bar{x}$ = 16 µm, $n_{sections}$ = 10). Ventral directives supported by mesoglea 219–250 µm ($\bar{x}$ = 232 µm, $n_{sections}$ = 10) from column to siphonoglyph, 8–44 µm ($\bar{x}$ = 16 µm, $n_{sections}$ = 10) width. Small lacunae resulting from dissolution of encrustations throughout column ectoderm and mesoglea (Figure 8B). Encircling sinus composed of round lacunae centered within the mesoglea (Figure 8B).

Cnidae. Mesenterial filaments contain species characteristic large penicilli (holotrichs) (Sinniger *et al.*, 2013).

Distribution. Occurring at 390–496 m in the Western Pacific (Hawaii) colonizing unidentified octocorals of the family Primnoidae (Sinniger *et al.*, 2013). Also observed in submersible and ROV videos at Makapu'u coral bed off Oahu, Hawaii (Sinniger *et al.*, 2013).

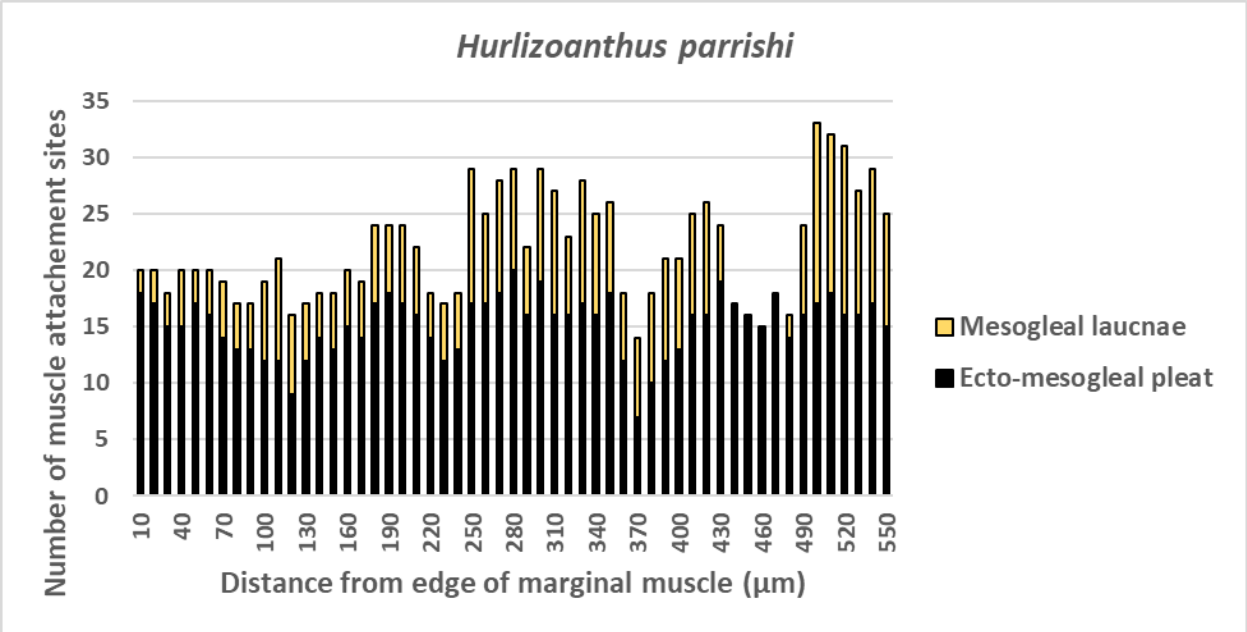

Figure 9. Number, position, and type of marginal muscle attachment sites as they appear in serial longitudinal sections of *Hurlizoanthus parrishi*. Individual columns represent a 10 µm longitudinal section with the number and type of muscle attachment points; black bars indicate ectodermal-mesogleal pleats, yellow bars indicate mesogleal lacunae.

Remarks. The original description of *Hurlizoanthus parrishi* did not report on the arrangement of the marginal musculature. The microanatomical analysis of *H. parrishi* in

Sinniger *et al.* (2013) lacks longitudinal and transverse serial sectioning. It appears that when viewing longitudinal serial sections of *H. parrishi* in sequence, the marginal musculature arrangement of the species can be described as cyclically transitional, consisting of a cyclic continuum of ectodermal-mesogleal pleats to a combination of ecto-mesogleal pleats and mesogleal lacunae, over a transition period of approximately 110–140 μm (Figure 9). This type of marginal musculature is congruent with the marginal musculature of species within the genera *Corallizoanthus* (Swain, 2010; Swain *et al.*, 2014) and similar to that of *Savalia savaglia* (Swain *et al.*, 2015).

Genus *Kauluzoanthus* Sinniger in Sinniger, Ocana & Baco, 2013

Type species. *Kauluzoanthus kerbyi* Sinniger in Sinniger, Ocana & Baco, 2013, by original designation.

Diagnosis. Characteristic insertion/deletion pattern in the 16S V5 mitochondrial region located in the second half of the mt16S rDNA gene, polyps not contracting when fixed (original diagnosis of Sinniger *et al.*, 2013). Marginal musculature cyclically transitional, 178–274 μm in length, composed of 5–23 attachment points (diagnosis expanded using data presented here).

Remarks. Genus *Kauluzoanthus* based almost entirely off characteristic insertion/deletion pattern in the 16S V5 mitochondrial region. Sinniger *et al.* (2013) provides no other delineating physical characteristics for the genus. Sinniger *et al.* (2013) describes polyps that do not contract when fixed. Out of the five genera-type species examined in this study, *Kauluzoanthus* exhibited the smallest marginal musculature length on average ($\overline{x}$ = 220 μm) and lowest amount of muscle attachments on average ($\overline{x}$ = 11), resembling a weak marginal musculature with the inability to easily contract. The original diagnosis has been expanded to include the marginal musculature arrangement (cyclically transitional). According to the original description of the family Parazoanthidae, taxa within this family are said to have simple endodermal marginal musculature (Delage & Hérouard, 1901). This is in direct contradiction with the findings of this research. Therefore, revision of Parazoanthidae is warranted.

***Kauluzoanthus kerbyi* Sinniger in Sinniger, Ocana & Baco, 2013**

Figure 10–11. Morphbank species collection F1084

Material examined. USNM 1190195, holotype.

Diagnosis: Polyps large, light beige, associated to *Kulumanamana haumeaae* (Sinniger *et al.*, 2013). Prescence of medium to large penicillin in the tentacles and body wall, special spirulae in tentacles characteristic of species (Sinniger *et al.*, 2013). Marginal musculature cyclically transitional, 178–274 µm in length, composed of 5–23 attachment points.

Colony. Thinly developed coenchyme partially covering *K. haumeaae* colonies as well as various octocoral species (Sinniger *et al.*, 2013). Colonial patches forming up to cm diameter with no host colony observed that was fully covered (Sinniger *et al.*, 2013).

Polyp. Polyps 1–5 mm in length and diameter, 23–28 pointed tentacles (Sinniger *et al.*, 2013). Polyps light beige *in vivo*, column cylindrical with no incrusted particles (Sinniger *et al.*, 2013).

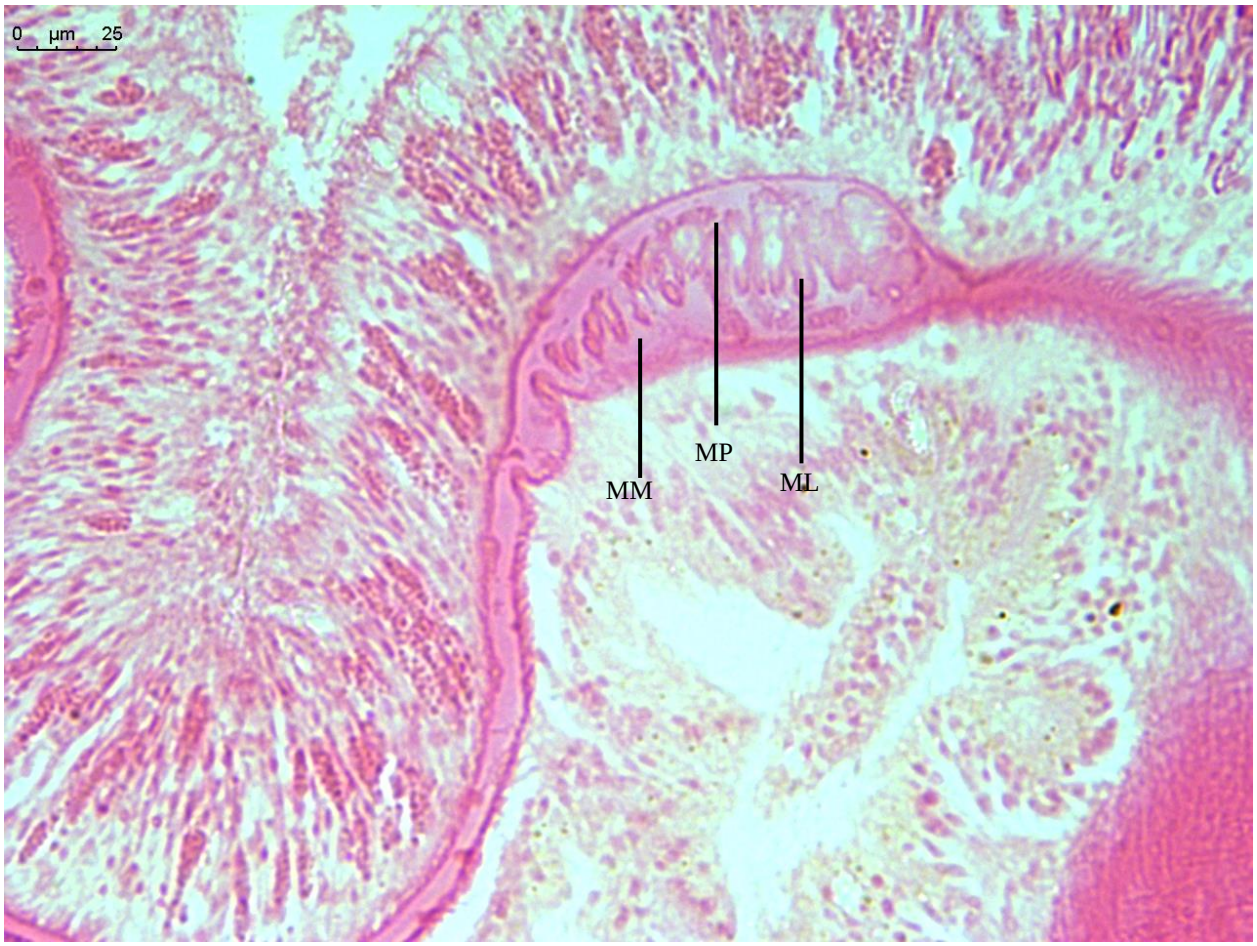

Figure 10. Histology of *Kauluzoanthus kerbyi* (10 µm sections). Longitudinal section showing marginal musculature (MM), mesogleal pleat (MP) and mesogleal lacunae (ML).

Internal anatomy. Azooxanthellate, 20–25 mesenteries following macrocnemic arrangement, no gonads observed, mesenteries difficult to observe due to short column length (Sinniger *et al.*, 2013)

In longitudinal sections (Morphobank collection F1084)**,** marginal musculature cyclically transitional, with a period of approximately 170–230 µm (Figure 11). Muscle fibers contained within 0–23 ($\overline{x}$ = 7, $n_{sections}$ = 50) mesogleal lacunae (Figure 10) that span entire mesoglea distally; lacunae restricted to endoderm proximally, with most-proximal lacunae opening to endoderm and forming 5–19 ($\overline{x}$ = 11, $n_{sections}$ =50) mesogleal pleats (Figure 10). Length of marginal musculature (Figure 10) 178–274 ($\overline{x}$ = 220 µm, $n_{sections}$ = 10); diameter of muscle at widest point 8–50 µm ($\overline{x}$ = 182 µm, $n_{sections}$ = 10). Large lacunae throughout ectoderm and mesoglea resulting from dissolution of encrustations (Figure 10).

Cross sections at the actinopharynx of *Kauluzoanthus kerbyi* were not obtained due to difficulty in sectioning and limited type material from USMN. The original description (Sinniger *et al.*, 2013) details the species having a deep and narrow siphonoglyph with no sphincter observed (Sinniger *et al.*, 2013). Retractor muscle and parietobasilar muscles minimally developed (Sinniger *et al.*, 2013).

Cnidae. Mesenterial filaments contain spirocysts, special spirulae, penicillin, holotrichs (Sinniger *et al.*, 2013). Cellular structures containing possible micronematocysts observed in body wall (Sinniger *et al.*, 2013).

Distribution. Found in Hawaiian archipelago with similar distribution as *Kulamanamana haumeaae*, other zoanthidea observed in other Pacific locations including Line, Jarvis, Palmyra, and Kingman (Sinniger *et al.*, 2013).

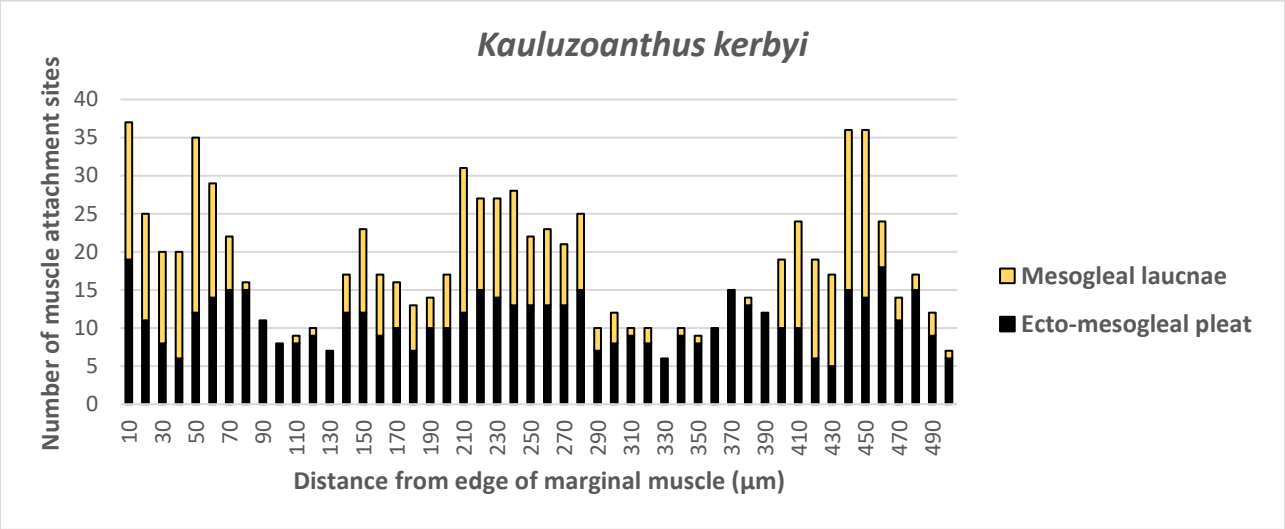

Figure 11. Number, position, and type of marginal muscle attachment sites as they appear in serial longitudinal sections of *Kauluzoanthus kerbyi*. Individual columns represent a 10 µm longitudinal section with the number and type of muscle attachment points; black bars indicate ectodermal-mesogleal pleats, yellow bars indicate mesogleal lacunae.

Remarks. The original description of *Kauluzoanthus kerbyi* reported the arrangement of the marginal musculature as "not observed." The microanatomical analysis of *K. kerbyi* in Sinniger *et al.* (2013) lacks longitudinal and transverse serial sectioning. It appears that when viewing longitudinal serial sections of *K. kerbyi* in sequence, the marginal musculature arrangement of the species is cyclically transitional, consisting of a cyclic continuum of ectodermal-mesogleal pleats to a combination of ecto-mesogleal pleats and mesogleal lacunae, over a transition period of approximately 170–230 µm (Figure 11). This type of marginal musculature is congruent with the marginal musculature of species within the genera *Corallizoanthus* (Swain, 2010; Swain & Swain, 2014) and similar to that of *Savalia savaglia* (Swain *et al.*, 2015).

Genus *Bullagummizoanthus* Sinniger in Sinniger, Ocana & Baco, 2013

Type species. *Bullagummizoanthus emilyacadiaarum* Sinniger in Sinniger, Ocana & Baco, 2013, by original designation.

Diagnosis. Characteristic insertion/deletion pattern in the 16S V5 mitochondrial region located in the second half of the mt16S rDNA gene (original diagnosis of Sinniger *et al.*,

2013). Marginal musculature cyclically transitional, 622–935 μm in length, composed of 8–21 attachment points (diagnosis expanded using data presented here).

Remarks. Genus *Bullagummizoanthus* based entirely off characteristic insertion/deletion pattern in the 16S V5 mitochondrial region. Sinniger *et al.* (2013) provides no delineating physical characteristics for the genus. The original diagnosis has been expanded to include the marginal musculature arrangement (cyclically transitional). According to the original description of the family Parazoanthidae, taxa within this family are said to have simple endodermal marginal musculature (Delage & Hérouard, 1901). This is in direct contradiction with the findings of this research. Therefore, revision of Parazoanthidae is warranted.

***Bullagummizoanthus emilyacadiaarum* Sinniger in Sinniger, Ocana & Baco, 2013**

Figure 12–13. Morphobank species collection F1087

Material examined. USNM 1190197, holotype.

Diagnosis. Colony distributed across entire host colony but does not cover entire host (Sinniger *et al.*, 2013). Polyp density low, associated with pargorgiid (Sinniger *et al.*, 2013). Prescence of special spirulae in the body wall and special penicillin in the filaments characteristic of this species (Sinniger *et al.*, 2013). Marginal musculature cyclically transitional, 622–935 μm in length, composed of 8–21 attachment points.

Colony. Poorly developed coenenchyme that does not completely cover the host (Sinniger *et al.*, 2013). Observed colony at least 30–40 cm in diameter, polyps sparsely distributed on the host, often in groups of few polyps issued of asexual reproduction (Sinniger *et al.*, 2013).

Polyp. In preserved specimens, contracted and semi-contracted polyps from 1–7 mm length and 2–7 mm diameter, 30–39 pointed tentacles (Sinniger *et al.*, 2013). Column cylindrical with incrusted mineral particles (sand, gorgonian sclerites) (Sinniger *et al.*, 2013). *In situ*, polyps bright yellow (Sinniger *et al.*, 2013).

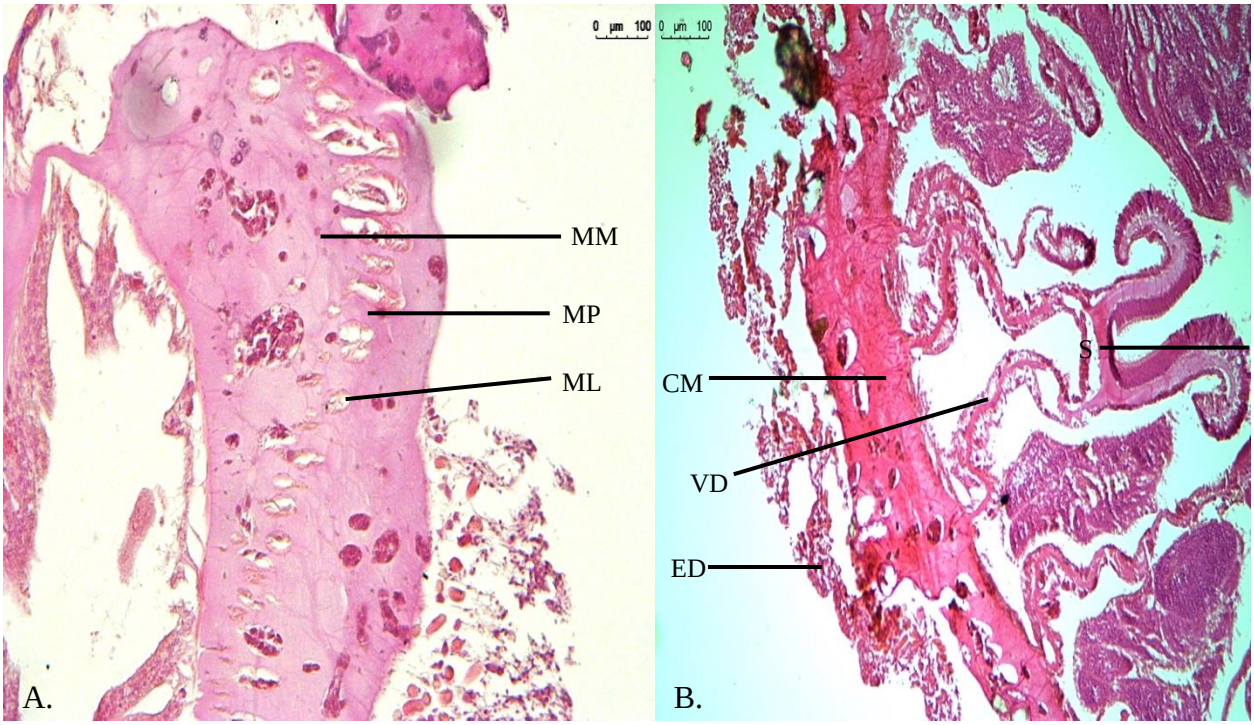

Figure 12. Histology of *Bullagummizoanthus emilyacadiaarum* (10 µm sections). **A.** Longitudinal section showing marginal musculature (MM), mesogleal pleat (MP) and mesogleal lacunae (ML). **B.** Transverse (cross) section showing a single siphonoglyph (S), column mesoglea (CM), ventral directive (VD) and column endoderm (ED).

Internal anatomy. Azooxanthellate, 30–40 mesenteries following macrocnemic arrangement with most mesenteries fertile regarding analyzed specimens (Sinniger *et al.*, 2013). Retractor muscle and parietobasilar muscle features went unnoticed, single conspicuous siphonoglyph (Sinniger *et al.*, 2013).

In longitudinal sections (Morphobank collection F1087), marginal musculature cyclically transitional, with a period of approximately 210 µm (Figure 13). Muscle fibers contained within 0–23 ($\bar{x}$ = 8, $n_{sections}$ = 53) mesogleal lacunae (Figure 12A) that span entire mesoglea distally; lacunae restricted to endoderm proximally, with most-proximal lacunae opening to endoderm and forming 8–21 ($\bar{x}$ = 15, $n_{sections}$ =53) mesogleal pleats (Figure 12A). Length of marginal musculature (Figure 12A) 622–935 ($\bar{x}$ = 546 µm, $n_{sections}$ = 10); diameter of muscle at widest point 147–261 µm ($\bar{x}$ = 182 µm, $n_{sections}$ = 12A). Large lacunae throughout ectoderm and mesoglea resulting from dissolution of encrustations (Figure 12A).

In cross sections at the actinopharynx (Morphobank collection F1087), mesenteries follow macrocnemic arrangement with a single siphonoglyph (Figure 12B). Thickness of

siphonoglyph ectoderm ranged from 20–40 µm ($\bar{x}$ = 27 µm, $n_{sections}$ = 10). Thickness of siphonoglyph mesoglea ranged from 12–27 µm ($\bar{x}$ = 19, $n_{sections}$ = 10). Thickness of siphonoglyph endoderm 22–40 µm ($\bar{x}$ = 30, $n_{sections}$ = 10). Adjacent siphonoglyph, column ectoderm thickness 66–156 µm ($\bar{x}$ = 114 µm, $n_{sections}$ = 10), mesoglea thickness 120–213 µm ($\bar{x}$ = 154 µm, $n_{sections}$ = 10), and endoderm thickness 20–51 µm ($\bar{x}$ = 29 µm, $n_{sections}$ = 10). Microneme 18–65 µm in length ($\bar{x}$ = 30 µm, $n_{sections}$ = 10), 4–14 µm in width ($\bar{x}$ = 8 µm, $n_{sections}$ = 10). Ventral directives supported by mesoglea 458–611 µm ($\bar{x}$ = 484 µm, $n_{sections}$ = 10) from column to siphonoglyph, 11–19 µm ($\bar{x}$ = 14 µm, $n_{sections}$ = 10) width. Small lacunae resulting from dissolution of encrustations throughout column ectoderm and mesoglea (Figure 12B). Encircling sinus composed of large round lacunae, irregularly occurring, central to the mesoglea (Figure 12B).

Cnidae. Mesenterial filaments containing spirocysts, special spirulae, special penicillin (new category of nematocysts, enlarged and incurved capsule with a thick filament full of spines inside), holotrichs (Sinniger *et al.*, 2013).

Distribution. Only colony observed was sub-sampled for description (Sinniger *et al.*, 2013). Similar zoanthideans have been frequently observed throughout the Pacific on samples of *Paragorgia coralloides* (Sinner *et al.*, 2013).

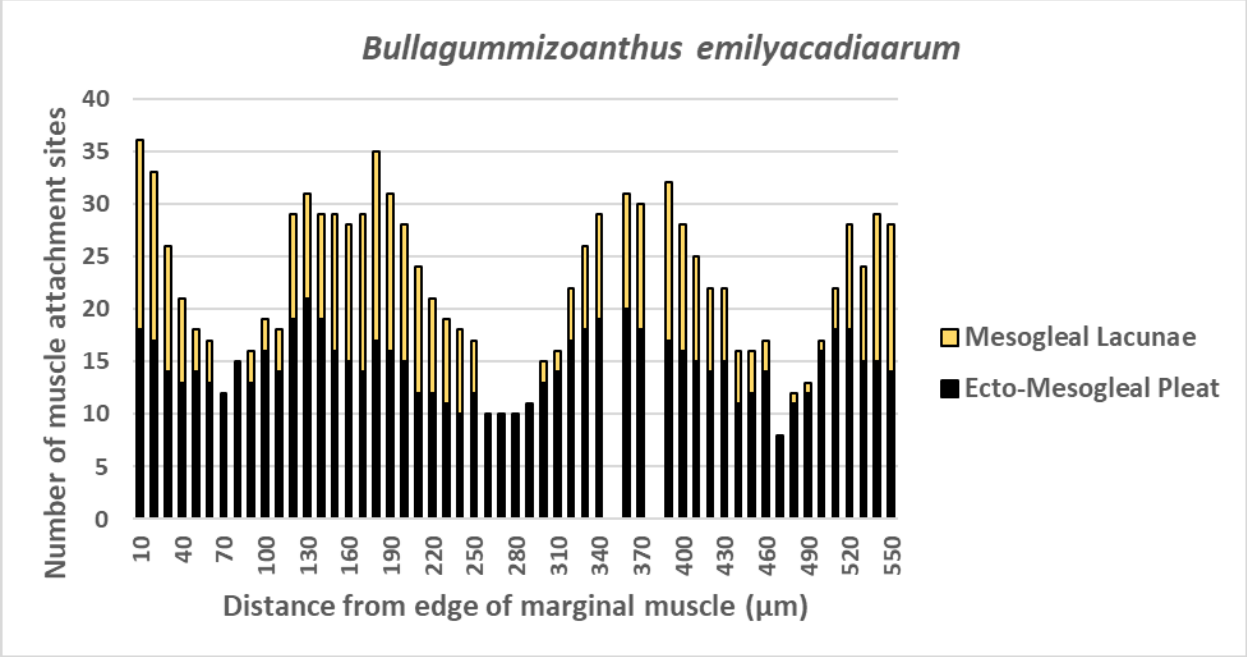

Figure 13. Number, position, and type of marginal musculature attachment sites as they appear in serial longitudinal sections of *Bullagummizoanthus emilyacadiaarum*. Individual columns represent a 10 µm longitudinal section with the number and type of muscle attachment points; black bars indicate ectodermal-mesogleal pleats, yellow bars indicate mesogleal lacunae. Empty positions indicate missing data due to sectioning artifact.

Remarks. The original description of *Bullagummizoanthus emilyacadiaarum* reported the arrangement of the marginal musculature incompletely, with the lone description as "weak endodermal sphincter" (Sinniger *et al.*, 2013). The microanatomical analysis of *B. emilyacadiaarum* in Sinniger *et al.* (2013) lacks longitudinal and transverse serial sectioning. It appears that when viewing longitudinal serial sections of *B. emilyacadiaarum* in sequence, the marginal musculature arrangement of the species can be described as cyclically transitional, consisting of a cyclic continuum of ectodermal-mesogleal pleats to a combination of ecto-mesogleal pleats and mesogleal lacunae, over a transition period of approximately 210 µm (Figure 13). This type of marginal musculature is congruent with the marginal musculature of species within the genera *Corallizoanthus* (Swain, 2010; Swain *et al.*, 2014) and similar to that of *Savalia savaglia* (Swain *et al.*, 2014).

Phylogeny

Attempts to extract DNA from each of the five genera type species (*Kulamanamana haumeaae,* USNM 1190188; *Zibrowius ammophilus,* USNM 1190192; *Hurlizoanthus parrishi,* USNM 1190194; *Kauluzoanthus kerbyi,* USNM 1190196; *Bullagummizoanthus emilyacadiaarum,* USNM 1190198) were unsuccessful. Protocols for DNA extraction outlined in Doyle & Doyle (1987) were unsuccessful in extracting genetic material from ethanol preserved type specimens. After multiple attempts with no success, the protocol outlined in Nyugen *et al.* (2021) was used based on the possibility that the type specimens were fixed in formalin. Following the failed attempt to extract DNA from the specimens using the formalin-based protocol, type material was exhausted.

Discussion

The formal taxon revisions presented here provide previously unexplored details on the marginal musculatures, siphonoglyph and adjacent structures (ventral directives, micronemes), and column wall parameters of five genera type species (*Kulamanamana haumeaae, Zibrowius ammophilus, Hurlizoanthus parrishi, Kauluzoanthus kerbyi, Bullagummizoanthus emilyacadiaarum*). With the addition of these microanatomical features to the original descriptions provided by Sinniger *et al.* (2013), our ability to identify these species and the

genera they represent is strengthened and our understanding of the evolution of form improved. These results provide identifiable characters that are independent of any molecular analysis, thus allowing previously collected specimens, in which genetic material may be inaccessible (as was the case here), to be identified and contextualized within the existing taxonomic system and modern phylogenetics. With the exception of transverse sections of *Kauluzoanthus kerbyi* and *Zibrowius ammophilus*, longitudinal and transverse sections were obtained for each type specimen and were uploaded to the morphology database, Morphobank. In addition to the expansion of each species description, genus descriptions were also expanded to include the marginal musculature arrangements for each specimen, with each species exhibiting a cyclically transitional marginal musculature arrangement. The original genus descriptions for each specimen provided little to no morphological details, with some (i.e. *Hurlizoanthus*, *Bullagummizoanthus*) being solely defined by a short insertion/deletion pattern in the 16S V5 mitochondrial region (Sinniger *et al.*, 2013). Additionally, each of the five genera analyzed in this research reside within the family Parazoanthidae. Taxa within this family are described as having simple endodermal marginal musculature (Delage & Hérouard, 1901) which directly contrasts findings of this and previous research. A cyclically transitional marginal musculature can be misinterpreted as simple endodermal when the musculature arrangement is assessed using a singular longitudinal section as opposed to serial sections viewed in sequence, which was conducted in this study. Therefore, based on my results and previous research, revision of the family Parazoanthidae is warranted.

The form of Zoanthidea marginal musculatures has been foundational in understanding the evolutionary relationships between higher taxa within the order for more than a century (Swain *et al.*, 2015). Described by Swain *et al.* (2015) as a possible morphological synapomorphy, varying marginal musculature forms may provide distinct character states capable of distinguishing between closely related higher taxa within the Zoanthidea. Sinniger *et al*. (2013), which described the five genera type species, did not report on the marginal musculature for three type species (*Kulamanamana haumeaae*, *Hurlizoanthus parrishi*, *Kauluzoanthus kerbyi*), and incorrectly reported that *Zibrowius ammophilus* and *Bullagummizoanthus emilyacadiaarum* exhibit a simple endodermal musculature. The form of the marginal musculature of each species analyzed in this study constituted a cyclically

transitional arrangement, which is the same arrangement of representatives within the genera *Corallizoanthus* and *Savalia* (Swain & Swain, 2014; Swain *et al.*, 2015). Due to the close phylogenetic relation of each of the five genera analyzed in this study to *Corallizoanthus* and *Savalia* (Swain, 2018), coupled with each genera exhibiting a cyclically transitional marginal musculature, it may be appropriate to place each of these species into either *Corallizoanthus* or *Savalia*, thus avoiding the erection of five novel genera in the Zoanthidea that are based on short regions in the mitochondrial 16S V5 region.

Attempts to extract genetic material from the five type museum specimen were unsuccessful (see methods). Thus, expanding on the molecular analysis in Sinniger *et al*. (2013) was not achieved. Difficulties in extracting genetic material for DNA sequencing from museum samples has been widely documented (Rohland *et al.*, 2007; Chakraborty *et al.*, 2006). The inability to extract any sequenceable material from museum type specimens could be due to a multitude of reasons, including (but not limited to) fixatives used, preservation time, storage temperature, and tissue origin (Chakraborty *et al.*, 2006). The preservation status of the five type specimen was clearly reported in the original publication (Sinniger *et al.*, 2013) and in the information provided to the USNM, indicating that a sub-sample from each type specimen was stored in 95% ethanol for genetic analysis. The museum identification numbers correlating with the ethanol-preserved type material were verified. Due to the scrupulous, repetitive application of the CTAB extraction protocol (Doyle & Doyle, 1987) & formalin-fixed protocol (Nyugen *et al*. 2021), the use of the same primers outlined in Sinniger *et al*. (2013), and the indicated preservation status of the type specimens, the failure of DNA extractions remains unresolved.

Despite the inability of this study to successfully incorporate genetic analyses of the five type specimens in order to reconstruct a comprehensive, multi-gene molecular phylogeny, observations on the evolution of form in the Zoanthidea can still be inferred by mapping physical characters onto existing phylogenies. Despite concerns in regards to the sole use of morphological characters to infer evolutionary history, using independently derived molecular phylogenies to analyze the evolution of morphology is broadly considered the optimal approach (Budd *et al*., 2010; Fukami *et al*., 2008; Swain *et al*., 2017). By utilizing two existing phylogenies from Swain (2018; Figure 1) and Carreiro-Silva *et al*. (2017: Figure 7), a composite

phylogeny can be utilized to map the marginal musculature arrangements of each type species analyzed in this study and other closely related species (i.e. *Corallizoanthus tsukaharai*, *Savalia savaglia* (Swain, 2015).

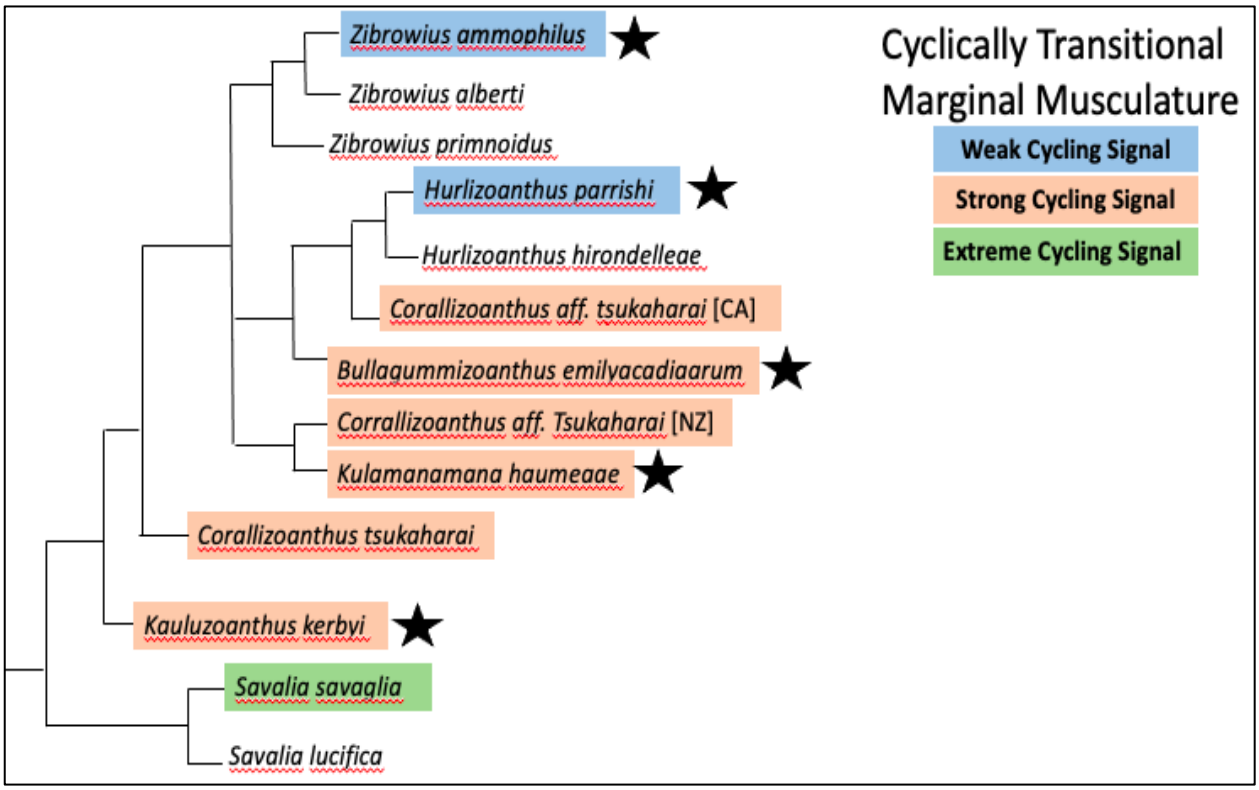

Figure 14. Composite phylogeny based on the molecular phylogenies of Swain (2018) and Carreiro-Silva *et al.* (2017), with species of known marginal musculatures highlighted. Cycling signal, interpreted from Figures 5, 7 , 9 ,11, 13 and Figure 2 from Swain *et al*. (2015), consist of three signal strengths; Extreme (*Savalia savaglia*), strong (*Kauluzoanthus kerbyi, Corallizoanthus tsukaharai, Kulamanamana haumeaae, Corallizoanthus aff. Tsukaharai* [NZ], *Corallizoanthus aff. Tsukaharai* [CA]), and weak (*Hurlizoanthus parrishi, Zibrowius ammophilus*). Marginal musculatures for *Savalia lucifica*, *Hurlizoanthus hirondelleae*, *Zibrowius primnoidus*, and *Zibrowius alberti* have not been assessed. Type specimens from Sinniger *et al*. (2013) indicated by adjacent black star.

Each species highlighted in figure 14 exhibits a cyclically transitional marginal musculature arrangement however, the transitions or cycles from ecto-mesogleal pleats to ecto-mesogleal lacunae varies across species, indicated by the respective column chart for each species presented in this study (figure 5, *Kulamanamana haumeaae*; figure 7, *Zibrowius ammophilus*; figure 9, *Hurlizoanthus parrishi*; figure 11, *Kauluzoanthus kerbyi*; figure 13, *Bullagummizoanthus emilyacadiaarum*). Each column chart is a quantification of the cycling between ecto-mesogleal pleats and ecto-mesogleal lacunae as viewed through serial longitudinal

sections in sequential order. Figures 5 (*Kulamanamana haumeaae*), 11 (*Kauluzoanthus kerbyi*), and 13 (*Bullagummizoanthus emilyacadiaarum*) display what is characterized as a strong cycling signal. Figures 7 (*Zibrowius ammophilus*) and 9 (*Hurlizoanthus parrishi*) display what is characterized as a weak cycling signal. *Savalia savaglia* exhibits an extreme cycling signal, transitioning from ecto-mesogleal pleats, through ecto-mesogleal lacunae, continuing to endo-mesogleal pleats (Swain *et al.*, 2015). Figure 14 appears to show the cycling signal or strength of the transition between different muscle attachment sites is decreasing during subsequent speciation events proceeding from the basal clade containing *Savalia savaglia.* As such, this may suggest that the evolution of the cyclically transitional marginal musculature has progressively shifted away from swift, abrupt changes in the musculature moving through serial sections of the polyp, towards less-pronounced cycles of ecto-mesogleal pleats and ecto-mesogleal lacunae in the marginal musculature.

In the original publication formally describing *Kulamanamana haumeaae*, *Zibrowius ammophilus*, *Hurlizoanthus parrishi*, *Kauluzoanthus kerbyi*, and *Bullagummizoanthus emilyacadiaarum*, Sinniger *et al*. (2013) provides four explanations for erecting these five genera: 1) based on close phylogenetic relatedness between all octocoral-associated species (including *Corallizoanthus sp.*), all species examined could be placed within *Savalia* or *Corallizoanthus*. However, *Savalia* is characterized by its ability to secrete a skeleton, an ability not shared by *Corallizoanthus*, *Hurlizoanthus parrishi*, and *Kauluzoanthus kerbyi* (and undetermined in *Zibrowius ammophilus*). The Hawaiian species may be placed within *Corallizoanthus*, with *Savalia* remaining independent, but *Kulamanamana haumeaae*'s skeleton secretion is difficult to disregard. 2) The morphology of the colonies between the species are significantly different. *Corallizoanthus* and *Bullagummizoanthus* colonies both separate during ontogeny, with the other species presenting dense colonies. 3) Skeleton secreting Zoanthideans could be placed within *Savalia*, however, the absence or presence of incrustations appears to be a significant character, equally as important as skeleton secretion is for differentiating between genera. 4) Each new species, sharing few characteristics and possessing their own distinct features should be placed in their own genus.

Since the publication of Sinniger *et al*. (2013), three species have been discovered or re-classified and placed within the novel genera erected in the 2013 publication. These include *Zibrowius primnoidus*, *Zibrowius alberti*, and *Hurlizoanthus hirondelleae* (Carreiro-Silva *et al*., 2017). Using the composite phylogeny (Figure 14), the rationale provided by Sinniger *et al*. (2013) can be analyzed by mapping the physical characters onto the phylogeny. The physical characters, shown in table 2, are: 1) skeleton secretion, 2) colony morphology, and 3) tissue incrustations.

Table 2. Compiled ancestral characters (skeleton secretion, colony morphology, tissue incrustations) of species from redrawn phylogeny of Swain (2018) and Carreiro-Silva *et al*. (2017).

Species	**Source**	**Character**		
		Skeleton Secretion 1 = No 2 = Yes	Colony Morphology 1 = Separates During Ontogeny 2 = Colonial	Tissue Incrustations 1 = None 2 = Incrusted
Zibrowius primnoidus	Carreiro-Silva *et al*. (2017)	1	2	2
Zibrowius alberti	Carreiro-Silva *et al*. (2017)	1	2	2
Zibrowius ammophilus	Sinniger *et al*. (2013)	Unknown	2	2
Hurlizoanthus hirondelleae	Carreiro-Silva *et al*. (2017)	Unknown	2	2
Hurlizoanthus parrishi	Sinniger *et al*. (2013)	1	2	2
Corallizoanthus aff. tsukaharai **[CA]**	Swain *et al*. (2015)	1	2	2
Bullagummizoanthus emilyacadiaarum	Sinniger *et al*. (2013)	1	1	2
Kulamanamana haumeaae	Sinniger *et al*. (2013)	2	2	1
Corallizoanthus aff. Tsukaharai **[NZ]**	Swain *et al*. (2015)	1	2	2
Corallizoanthus tsukaharai	Reimer *et al*. (2008)	1	1	2
Kauluzoanthus kerbyi	Sinniger *et al*. (2013)	1	2	1
Savalia savaglia	Lacaze-Duthiers (1864)	2	2	2
Savalia lucifica	Cutress & Pequegnat (1960)	1	2	2

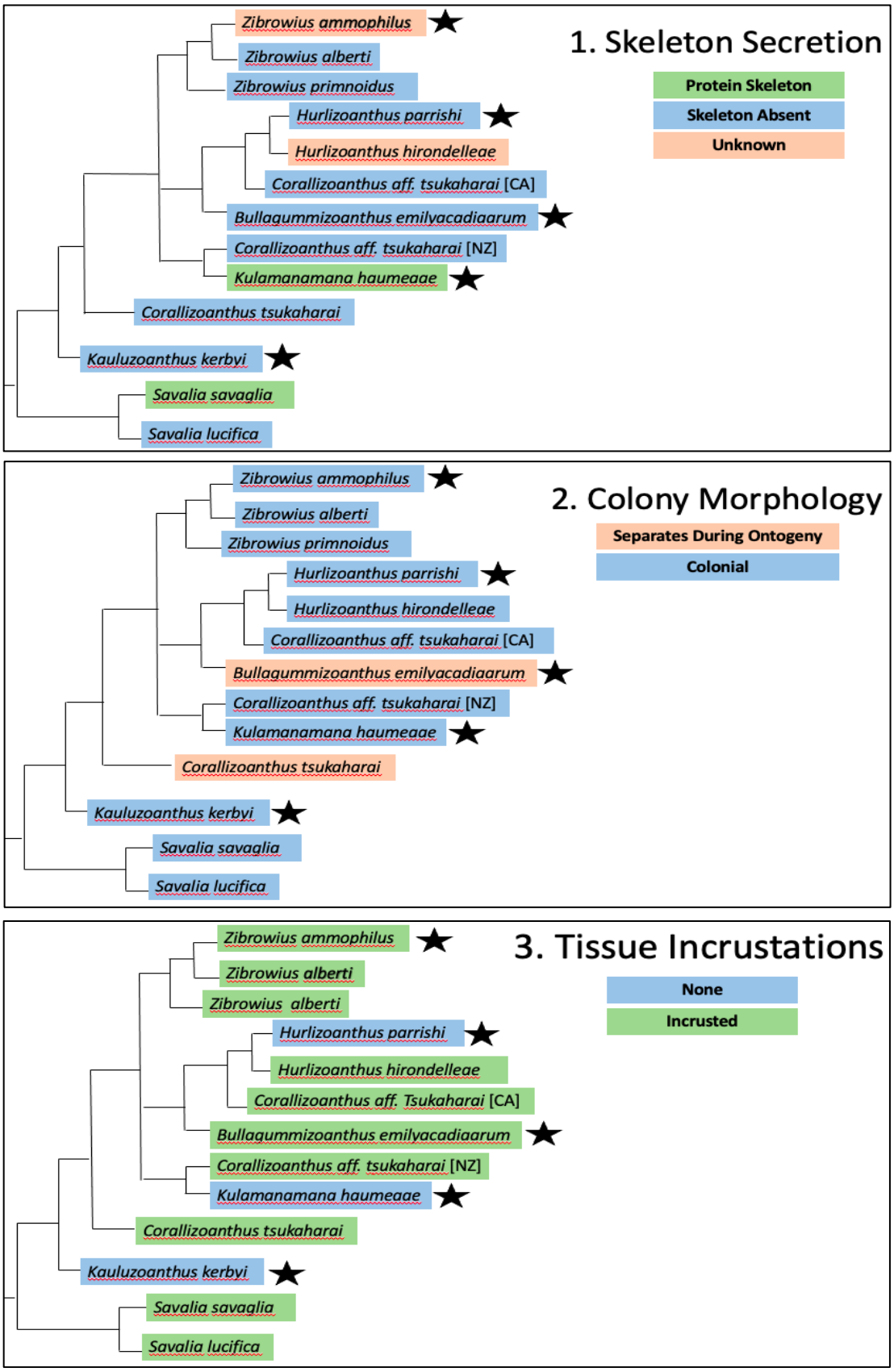

Figure 15. Physical characters mapped onto redrawn phylogeny of Swain (2018) and Carreiro-Silva et al. (2017). Characters include skeleton secretion (1), colony morphology (2), and tissue incrustations (3). Type species from Sinniger *et al.* (2013) indicated by adjacent black star.

According to the original justification provided by Sinniger *et al*. (2013), that octo-coral associated species can be placed within *Savalia* or *Corallizoanthus* depending on the secretion of a protein skeleton, Figure 15.1 suggests that species not producing their own protein skeleton are not disqualified from the genus *Savalia*. The original species description of *Savalia lucifica* provides no evidence of this species secreting a protein skeleton (Cutress & Pequegnat, 1960). Skeleton secretion is a difficult character to assess within the Zoanthidea, because it is difficult to observe and differentiate between a skeleton that has been created by the host and one created by the symbiont. Additionally, *Kulamanamana haumeaae*'s close phylogenetic relation to *Corallizoanthus aff. tsukaharai* [NZ], a non-skeleton secreting species, suggests that skeleton secretion within the Zoanthidea may not constitute a synapomorphic character trait. Therefore, based on the close phylogenetic relation of all octo-coral associated species, each type species from Sinniger *et al*. (2013) could have been placed within *Savalia* or *Corallizoanthus*. As it pertains to the notion that colony morphology is significantly different across the species represented in the composite phylogeny, this holds true for *Corallizoanthus tsukaharai* and *Bullagummizoanthus emilyacadiaarum* (Figure 15.2), both exhibiting colony separation during development. However, the remaining species represented remain colonial throughout their development. When viewing the phylogeny, colony morphology also does not appear to be synapomorphic. Lastly, as it pertains to tissue incrustations (Figure 15.3), this character trait also does not appear to be synapomorhpic within the phylogeny. Based on the analysis of the rationale provided by Sinniger *et al*. (2013) within the context of new data, the decision to erect five new monospecific genera rather than place the species within an existing genus (such as *Savalia* or *Corallizoanthus*) is not supported. Despite the questionable need for genera *Kulamanamana, Zibrowius, Hurlizoanthus, Kauluzoanthus*, and *Bullagummizoanthus*, they have been established within Zoanthidea systematics and new species have been placed in some of these genera. Without substantial new molecular evidence to further support or refute the prior classifications by Sinniger *et al*. (2013), it remains to be seen if these higher taxa should be revised.

Through this research, the expansion of five genera and species descriptions was achieved by expanding the morphological analysis conducted by Sinniger *et al*. (2013) to include marginal musculature assessments for each type specimen, all of which constituted a cyclically

transitional marginal musculature arrangement. With the addition of critical morphological characters to the existing molecular parataxonomic descriptions, each type specimen analyzed was reconnected to the existing Zoanthidea taxonomic system, providing useful characters for future research, independent of molecular techniques. All longitudinal and transverse histology sections for each species analyzed in this research are now publicly available through the public morphology database, Morphobank. To validate or refute the diagnoses regarding the genera designations of these type specimens, further molecular phylogenetic analysis is needed to resolve outstanding questions.

References

Abel, E.F. (1959). Zur Kenntnis der marinen Höhlenfauna unter.besonder Berücksichtigung der Anthozoen. *Pubblicazioni della Stazione zoologica di Napoli, 30*, 1–94.

Appeltans W, Ahyong Shane T, Anderson G, Angel Martin V, Artois T, Bailly N, Bamber R, Barber A, Bartsch I, Berta A, et al. 2012. The Magnitude of Global Marine Species Diversity. *Current Biology*, 22:2189–2202.

Brower AVZ. 2006. Problems with DNA barcodes for species delimitation: 'Ten species' of *Astraptes fulgerator* reassessed (Lepidoptera: Hesperidae). *Systematics and Biodiversity,* 4: 127–132.

Budd, A. F., Romano, S. L., Smith, N. D. & Barbeitos, M. S. (2010). Rethinking the phylogeny of scleractinian corals: a review of morphological and molecular data. *Integrative and Comparative Biology, 50*, 411–427.

Carreiro-Silva M, Braga-Henriques A, Sampaio I, de Matos V, Porteiro FM, Ocaña O. 2011. Isozoanthus primnoidus, a new species of zoanthid (Cnidaria: Zoantharia) associated with the gorgonian Callogorgia verticillata (Cnidaria: Alcyonacea). *Ices Journal of Marine Science*, 68:408–415.

Carreiro-Silva M, Ocaña O, Stankovic D, Sampaio Í, Porteiro FM, Fabri M-C, Stefanni S. 2017. Zoantharians (Hexacorallia: Zoantharia) Associated with Cold-Water Corals in the Azores Region: New Species and Associations in the Deep Sea. *Frontiers in Marine Science*, 4:88.

Chakraborty, A., Sakai, M., & Iwatsuki, Y. (2006). Museum fish specimens and molecular taxonomy: a comparative study on DNA extraction protocols and preservation techniques. *Journal of Applied Ichthyology*, *22*(2), 160-166.

Chen CA, Wallace CC, Wolstenholme J. 2002. Analysis of the mitochondrial 12S rRNA gene supports a two-clade hypothesis of the evolutionary history of scleractinian coral. *Molecular Phylogenetics and Evolution*, 23:137–149.

Collins RA & Cruickshank RH. 2013. The seven deadly sins of DNA barcoding. Molecular Ecology Resources 13:969–975.

Cutress, C. E.; Pequegnat, W. E. (1960). Three new species of Zoantharia from California. *Pacific Science.* 14, 89-100.

Dayrat, B. (2005). Towards integrative taxonomy. *Biological journal of the Linnean Society, 85*(3), 407–415. doi:https://doi.org/10.1111/j.1095-8312.2005.00503.x

Desalle, R., Egan, M.G. & Siddall, M. (2005). The unholy trinity: taxonomy, species delimitation and DNA barcoding. *Philosophical Transactions of the Royal Society B: Biological Sciences*, 360, 1905–1916.

Delage, Y. & Hérouard, E. (1901) Zoanthidés. – Zoanthidae. *In: Trait de Zoologie conrète. Tome II – 2me partie. Les Coelentérés*. C. Reinwald, Paris, pp. 654–667.

Doyle JJ, Doyle JL. 1987. A rapid DNA isolation procedure for small quantities of fresh leaf tissue. In.

Haddon, A.C., & Shackleton, A. M. (1891). A revision of the British actiniae Part II: The Zoanthidae. *The Scientific Transactions of the Royal Dublin Society 4.*

Lacaze-Duthiers, H. (1864). Mémoire sur les antipathaires (genre Gerardia, L. D.). Annales des Sciences Naturelles, 2, 5th, 169-239
page(s): 169-239.

Lipscomb D, Platnick N, Wheeler Q. 2003. The intellectual content of taxonomy: a comment on DNA taxonomy. Trends in Ecology & Evolution 18:65–66.

Nguyen, H.T., Tatipamula, Do, D.N., Huynh, T.C., Dang, M.K. (2021). Retrieving high-quality genomic DNA from formalin-fixed paraffin-embedded tissues for multiple molecular analyses. *Preparative Biochemistry & Biotechnology*, doi:10.1080/10826068.2021.1923030

Padial, J. M., Miralles, A., De la Riva, I., & Vences, M. (2010). The integrative future of taxonomy. *Frontiers in Zoology*, *7*(1), 16. doi:10.1186/1742–9994–7–16

Pante, E., Puilandre, N., Viricel, A., Arnaud-Haond, S., Aurelle, D., Castelin, M., Chenuil, A., Destombe, C., Forcioli, D., Valero, M., Viard, F. & Samadi, S. (2015). Species are hypotheses: avoid connectivity assessments based on pillars of sand. *Molecular Ecology, 24, 525–544.*

Reimer, J.D., Hirano, S., Fujiwara, Y., Sinniger, F. & Maruyama, T. (2007). Morphological and molecular characterization of *Abyssoanthus nankaiensis*, a new family, new genus and new species of deep-sea zoanthid (Anthozoa: Hexacorallia: Zoantharia) from a northwest Pacific methane cold seep. *Invertebrate Systematics*, 21, 255–262. http://dx.doi.org/10.1071/is06008

Reimer JD, Ono S, Takishita K, Tsukahara J, Maruyama T. 2006. Molecular Evidence Suggesting Species in the Zoanthid Genera *Palythoa* and *Protopalythoa* (Anthozoa: Hexacorallia) Are Congeneric. Zoological Science 23:87–94, 88.

Rohland, N., & Hofreiter, M. (2007). Comparison and optimization of ancient DNA extraction. *Biotechniques*, *42*(3), 343-352.

Ryland J, Lancaster J. 2004. A review of zoanthid nematocyst types and their population structure. *Hydrobiologia*, 530: 179.

Schmidt, O. (1862). Die spongien des Adriatischen Meeres. *Wilhelm Engelmann: Leipzig, i-viii.*

Shearer T, Van Oppen M, Romano S, Wörheide G. 2002. Slow mitochondrial DNA sequence evolution in the Anthozoa (Cnidaria). *Molecular ecology*, 11:2475–2487.

Sinniger F, Ocana OV, Baco AR. 2013. Diversity of zoanthids (Anthozoa: Hexacorallia) on Hawaiian seamounts: description of the Hawaiian gold coral and additional zoanthids. *PLoS ONE* 8(1), e52607.

Sinniger F, Montoya-Burgos JI, Chevaldonne P, Pawlowski J. 2005. Phylogeny of the order Zoantharia (Anthozoa, Hexacorallia) based on the mitochondrial ribosomal genes. *Marine Biology* 147: 1121–1128.

Sinniger, F., Reimer, J.D. & Pawlowski, J. (2010). The Paraxoanthidae (Hexacorallia: Zoantharia) DNA taxonomy: description of two new genera. *Marine Biodiversity*, 40, 57–70.

Swain, T. D., & Wulff, J. L. (2007). Diversity and specificity of Caribbean sponge-zoanthid symbioses: a foundation for understanding the adaptive significance of symbioses and generating hypotheses about higher-order systematics. *Biological Journal of the Linnean Society*, 92(4), 6950711. doi:10.1111/j.1095-8312.2007.00861.x

Swain TD. 2010. Evolutionary Transitions in Symbioses: Dramatic Reductions in Bathymetric and Geographic Ranges of Zoanthidea Coincide with Loss of Symbioses with Invertebrates. *Molecular Ecology*, 12: 2587–2598.

Swain. T. 2009. Phylogeny-based species delimitations and the evolution of host associations in symbiotic zoanthids (Anthozoa, Zoanthidea) of the wider Caribbean region. *Zoological Journal of the Linnean Society*, 156:223–238.

Swain TD, Schellinger JL, Strimaitis AM, Reuter KE. 2015. Evolution of Anthozoan Polyp Retraction Mechanisms: Convergent Functional Morphology and Evolutionary Allometry of the Marginal Musculature in Order Zoanthidea (Cnidaria: Anthozoa: Hexacorallia). *BMC Evolutionary Biology*, 123:1–19.

Swain T, Swain L. 2014. Molecular parataxonomy as taxon description: Examples from recently name Zoanthidea (Cnidaria: Anthozoa) with revision based on serial histology of microanatomy. *Zootaxa*, 3796:81–107.

Swain TD. 2018. Revisiting the phylogeny of Zoanthidea (Cnidaria: Anthozoa): Staggered alignment of hypervariable sequences improves species tree inference. *Molecular Phylogenetics and Evolution*, 118:1–12.

Swain TD, Strimaitis AM, Reuter KE, Boudreau W. 2017. Towards integrative systematics of Anthozoa (Cnidaria): evolution of form in the order Zoanthidea. *Zoologica Scripta*, 46:227–244.

Vogler AP, Monaghan MT. 2007. Recent advances in DNA taxonomy. *Journal of zoological systematics and evolutionary research*, 45:1–10.

Will, K. W., Mishler, B. D. & Wheeler, Q. D. (2005). The perils of DNA barcoding and the need for integrative taxonomy. *Systematic Biology*, *54*, 844-851.

Zamani A, Fric ZF, Gante HF, Hopkins T, Orfinger AB, Scherz MD et al. 2022. DNA barcodes on their own are not enough to describe a species. *Systematic Entomology*, 1–5.